

WIND TUNNEL MODEL TESTS TO INVESTIGATE  
THE EFFECTS OF BOUNDARY LAYER CONTROL

Thesis

by

I. L. Ashkenas and R. B. Smith

In Partial Fulfillment of the  
Requirements for the Degree of Master of Science  
in Aeronautics  
California Institute of Technology  
Pasadena, California

1939

## ACKNOWLEDGEMENT

The authors wish to express their thanks and appreciation to Drs. Clark B. Milliken, and William R. Sears and to Mr. L. B. Rumph, Jr. for their interest in the problem and their helpful suggestions throughout the course of the research.

Further thanks are expressed to the members of the wind tunnel crew for their willing help in carrying out the tests.

## TABLE OF CONTENTS

	PAGE
ACKNOWLEDGEMENT	1
TABLE OF CONTENTS	1
NOTATION	2
SUMMARY	4
INTRODUCTION	5
EXPERIMENTAL PROCEDURE	
DESCRIPTION OF MODEL	7
DESCRIPTION OF TESTS	10
REDUCTION OF DATA	12
DISCUSSION OF RESULTS	15
REFERENCES	23
FIGURES	24
APPENDIX I	I
APPENDIX II   MODEL WITH GRID	IV

## NOTATION

$\alpha$	Angle of attack of model with reference to chord line
AR	Aspect Ratio
a.c.	Aerodynamic center
b	Wing span
B	Fuselage of model
$CD_p^i$	"Ideal" parasite drag coefficient
$CD_p$	"Equivalent" parasite drag coefficient = $CD_p^i + CD_s$
$CD_R$	Coefficient giving drag reaction on model due to air flowing through it
$\Delta CM_R$	Coefficient giving moment reaction on model due to air flowing through it
$CD_s$	Measure of power used to remove boundary layer = $\frac{E}{qSV}$
$CD_s^i$	= $CD_s - C_Q$
$C_L$	Lift coefficient
$C_Q$	Measure of quantity of air handled per second = $\frac{Q}{SV}$
E	Power supplied to air passing through Boundary Layer Model
F	Flap - a 20% chord split flap set at 45° and covering practically the full span except for the fuselage.
G	Slot in wing - subscript indicates specific slot
H	Total head of flow
$\theta$	Angle of exhaust jet to undisturbed velocity
q	Dynamic pressure in the tunnel during the test
Q	Quantity of air passing through model per second
$\rho$	Density
RN	Reynolds Number

S Wing area  
t Mean aerodynamic chord  
V Undisturbed velocity in the tunnel  
V<sub>e</sub> Exit velocity of jet  
W Wing of model

## SUMMARY

This thesis presents a study of the results obtained with the Boundary Layer Removal Model of the Guggenheim Aeronautics Laboratory, California Institute of Technology (GALCIT). It is a continuation of work begun here some time past and, as such, contains very little in the way of historical review, the origin of the project, preliminary studies of the problem and experimental technique being contained in previous reports.

The attempt, in this series of tests, to find a definite scale effect on the power required to produce a given change in airfoil characteristics has been somewhat unsuccessful because the test Reynolds Numbers unfortunately fell in the region of critical Reynolds Number. There has, however, been some success in finding the definite mechanism by which boundary layer removal is effective, a logical explanation being given for the nature and magnitude of various changes in airfoil characteristics incurred by the use of a given amount of suction.

## INTRODUCTION

The possibilities of approximating perfect fluid flow by some means of boundary layer control have been under investigation since the introduction of the boundary layer concept by Prandtl in 1904. Unfortunately, technological difficulties with the apparatus involved have delayed experimenters and prevented the accumulation of comparable data; with the result that conclusions as to the effectiveness of boundary layer control are as numerous as the number of experiments themselves. The difficulty in correlating various experiments lies in the number of variables involved. The most important of these are:

1. Airfoil Section
2. Wing Plan-form
3. Reynolds Number
4. Slot location
5. Slot size
6. Slot shape
7.  $C_Q$
8.  $C_{D_S}$

The first three of these parameters vary with each experiment, with the result that correlation, on ordinary bases, is very unsuccessful, and will probably only be attained through comparison of a non-geometrical parameter, such as the pressure gradient over the upper surface of the wing.

While this confusion as to the quantitative effects of boundary layer control exists, there is little doubt as to the qualitative results obtained. The accumulated experience of previous research indicates that, in general:

1) Removing the boundary layer by suction requires less power to produce a given effect than accelerating it with a jet.

2) Thick wings permit greater improvement through boundary layer control than do thin ones.

In the case of boundary layer removal:

3) Slot size and shape is unimportant except in determining the amount of power required to move the air.

4) A single slot is more efficient than multiple slots.

5) The optimum slot location is from 40% to 70% of the chord.

6) The general effects of applying suction are an increase in the maximum lift coefficient, an increase in the slope of the lift curve, and a decrease in parasite drag of the wing profile.

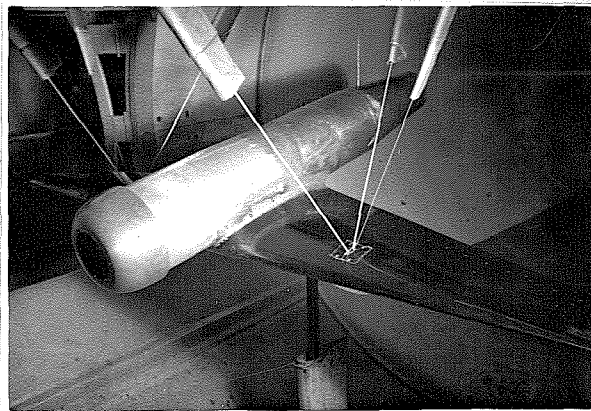
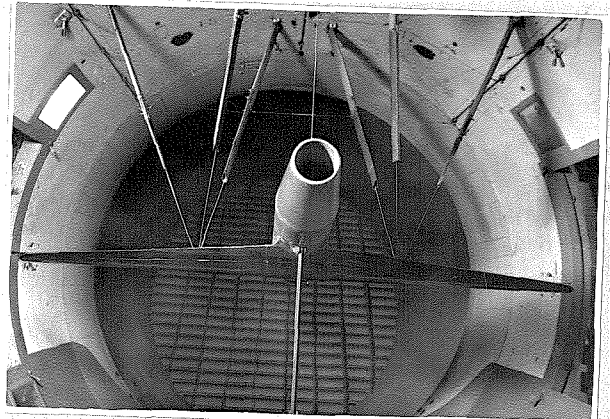
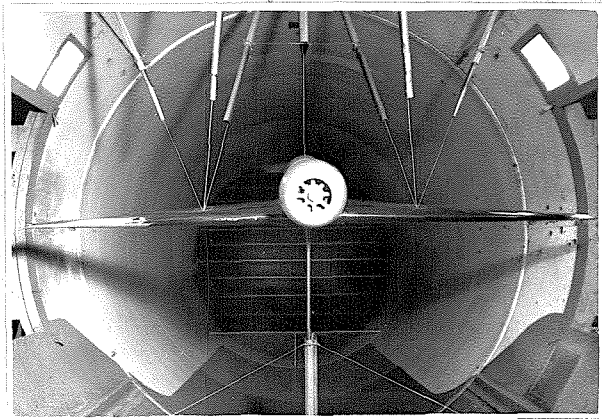
With these results in mind, tests have been made on the GALCIT model in an effort, primarily, to obtain high lift coefficients. The comparison of our most recent results with those obtained by others is shown in Figure 3 and, taking into account the variation in wing section and planform, indicates fair success.



## EXPERIMENTAL PROCEDURE

### DESCRIPTION OF MODEL

The GALCIT Boundary Layer Model, as tested, represents the wing and fuselage of a high wing monoplane. Its general appearance is shown in the photographs.



The air, which is removed from the upper surface of the wing and drawn down through the hollow wing, is exhausted through the tail of the fuselage.

The wing of the model is constructed of a channel-shaped aluminum alloy casting to which a copper sheet, forming the upper surface of the wing, is fastened. The slots, through which the air is sucked, are cut in this copper sheet and are located as shown in Figure 1. Slot  $G_3$  is placed at 70% of the chord and is .21" wide while the second slot tested,  $G_4$ , is .25" wide and is located along the 43% chord line. It should be stated here, for the benefit of those who may conduct further experiments on this model, that, as the model is now constructed, it is not possible to cut a slot between the 43% and the 65% point, due to a steel stringer under the copper sheet. If a slot is desired in this region it will be necessary to replace the upper surface of the wing with a new copper sheet. The trailing edge of the wing from 70% of the chord aft is made of wood as are the wing tips.

The dimensions of the wing are as follows:

Span	8 ft.
Aspect ratio	8.69
Area	7.36 sq. ft.
Mean Aerodynamic chord	11.02 in.
Taper ratio	4 to 1

The wing profile is shown in Figure 2

The circular fuselage of the model houses a 10 H.P. induction motor in front of the wing, connected to a two-stage axial flow fan located behind the wing.

The motor speed is controlled by a variable frequency set and speeds up to 18,000 R.P.M. are available. Pressures within the model are obtained through two piezometer rings, one located in front of and the other just behind the fan, and a pitot-static rake located in the exhaust jet in the tail of the fuselage. The difference in the static pressures at the two piezometer rings gives the pressure rise across the fan, and the pitot-static rake gives the average velocity in the exhaust and has been calibrated to give the quantity of air passing through the model. (See reference 2 for the details of this calibration.)

The model is rigged in the normal fashion for the GALCIT tunnel except that the counterweight wire is replaced by a streamlined strut which carries the electrical and pressure leads out of the tunnel.

DESCRIPTION OF TESTS

The procedure in making the various test runs was as follows:

Holding tunnel speed constant, the blower power was adjusted until a given quantity of air flow, as measured by the pitot rake, was obtained. The model was then set at various degrees of incidence, the air flow being kept constant, and the normal balance readings taken for these angles. This procedure was repeated for various blower powers at the given "q" and then the entire routine was repeated for each of the other tunnel speeds tested. In addition to balance readings, the static pressures in front of and behind the fan were also recorded.

The first few runs attempted disclosed the fact that one wing tip stalled approximately four degrees before the other without suction and six degrees with suction. This undesirable condition was finally eliminated, after an appreciable loss of time and a long series of tuft runs, by the discovery that the offending wing tip could be improved if the leading edge were made more blunt. A symmetrical stall was finally obtained by building up the leading edge of the bad wing tip with balsa wood, Durotite and paint. From this point on the tests ran quite smoothly, except for two bearing failures which not only reduced the amount of testing time, but also increased the apprehension of the operators, with the result that runs were made as quickly and with as few "extraneous" points as was thought feasible.

//

The configuration, WBG3, was first run at q's of 35, 25, 15, and 7 GMS/CM<sup>2</sup> without and with various amounts of suction, up to the maximum obtainable at each q. Next a 20% split flap was added and a series of suction runs made at a q of 7. Slot G<sub>4</sub> was then cut in the wing and, G<sub>3</sub> being covered with cellophane tape, a similar series was run. The final group of runs, intended to indicate the effect of slot configuration, was made at a constant C<sub>Q</sub> and q = 7 and included different arrangements of the two slots, made by taping over various portions of each.

## DATA REDUCTION TECHNIQUE

Removing the boundary layer required the use of two new parameters:  $C_Q$ , the quantity coefficient, and  $C_{DS}$ , the power coefficient. Their defining equations are:

$$C_Q = \frac{Q}{VS}$$

$$C_{DS} = \frac{E}{q VS}$$

Where  $Q$  = Quantity of air handled per second

$E$  = Power supplied to air

$V$  = Tunnel or free stream velocity

$q$  = Dynamic pressure

$S$  = Wing area

$E = Q(\Delta H)$ , and since for the GALCIT model

$\Delta H$  is measured directly as a pressure drop,  $\Delta P$ , plus the dynamic head corresponding to exit velocity (neglecting duct losses.)

$$C_{DS} = \frac{Q(\Delta P + \frac{1}{2}\rho V_e^2)}{VSq} = C_Q \left( \frac{\Delta P}{q} + \frac{V_e^2}{V^2} \right)$$

Thus  $C_Q$  is a non-dimensional measure of the quantity of air removed, while  $C_{DS}$  is a measure of the energy supplied to the air, giving no indication of the actual blower power required.

Assuming that the blower operates at the same efficiency as the propellor, it can be shown\* that the total drag will be a minimum if  $\frac{V_e}{V} = 1$ . Thus the "ideal" power coefficient is defined:

$$C_{DS} = C_Q \left( \frac{\Delta P}{q} + 1 \right) = C_{DS}' + C_Q$$

In addition to these parameters which are general for any boundary layer control model, the GALCIT model requires the

\* See Reference 9

application of certain corrections. The forces measured by the balance system include the drag associated with the intake of a certain quantity of air, and the thrust associated with the exhaust of the same quantity at a different velocity. The drag increase due to the intake of a quantity of air Q at tunnel velocity V is  $\rho QV$ . Similarly the exhaust thrust is  $\rho QV_e$ . Taking into account the inclination of the exhaust jet to the free stream velocity, the increased drag coefficient, due to the flow through the model is:

$$C_{DE} = \frac{\rho QV - \rho QV_e \cos \theta}{\frac{1}{2} \rho V^2 S}$$

$$C_{DE} = 2C_Q (1 - \frac{V_e}{V} \cos \theta)$$

Subtracting this quantity from the measured parasite drag gives the "ideal" parasite drag of the model which would correspond to the measured parasite drag if the thrust term in the above equation were equal to the drag term. Thus:

$$C_{DP}' = C_{DMEASURED} - \frac{C_L^2}{\pi AR} - C_{DE}$$

Since now  $C_{DP}$  is normally a measure of the power required for level flight, it is convenient to define an "equivalent" profile drag which includes the power input to the blower.

$$C_{DP} = C_{DP}' + C_{DS}$$

$C_{DP}$  now corresponds to the flat plate area normally associated with performance estimates.

The moment correction due to the eccentricity, e, of the exhaust jet about the reference point is obviously given by:

$$M_e = e \rho Q V_e$$

$$\Delta C_{Me} = \frac{e \rho Q V_e}{\frac{1}{2} \rho V^2 S t} = 2C_Q \frac{e}{t} \frac{V_e}{V}$$

The sign of this correction depends on the sign of e, e being measured positive along the positive Z axis. Then:

$$C_M = C_{M,MEASURED} - \Delta C_{MR}$$

The pitching moment thus includes the "sink" effect of the intake.



DISCUSSION

The mechanisms by which suction on the upper surface of a wing improve its aerodynamic characteristics are the following:

1) Superposition of the flow due to a sink on the normal flow pattern of the airfoil.

2) Introduction of a favorable pressure gradient on the upper surface of the wing and the consequent decrease in boundary layer thickness, and

3) The approach to ideal fluid flow because of the decreased boundary layer thickness.

These effects account for the general results observed in this as well as other experiments. These are, as mentioned before, an increase in maximum lift, an increase in slope of the lift curve, a decrease in drag, and a stabilizing effect on wing moment. The purpose of the following sections is to discuss the observed experimental results in the light of these effects.

1. LIFT

Because of the similar nature of all the experimental lift curves it is advisable to confine the discussion of the effect of suction on lift to the case of slot G3 at a q of 7 gms/cm<sup>2</sup>. This series is altogether typical and covers the widest range of C<sub>Q</sub>'s. A study of the lift curves corresponding to this configuration, (Figure 4) shows that, contrary to expectations, stall with suction occurs at approximately the same angle of attack as stall without suction. This result is contrary to theoretical considerations which indicate that, with the introduction

of a favorable pressure gradient, separation should be delayed and the stall should therefore occur at a higher angle of attack. This discrepancy is due, the authors feel, to the employment of such a highly tapered wing and the tendency of such wings to tip-stall; a tendency which was not removed by the application of suction, as revealed by flow investigation with tufts.

The increase in maximum lift coefficient is thus due entirely to the increase in slope of the lift curve and the change of angle of zero lift with suction. The increased slope of the lift curve with increasing suction may readily be accounted for by considering it a manifestation of the approach to perfect fluid flow. Thus, as is to be expected, a greater suction, because of its correspondingly greater decrease in boundary layer thickness, results in a closer approximation to the ideal slope of the lift curve. Considering the two extreme cases observed, and basing wing efficiency factors on the theoretical  $\frac{dC_L}{d\alpha}$  of a thick infinite AR wing\*, the wing efficiency was increased from 70.2% for the case of no suction to 88.6% at a  $C_Q = .0189$ ; the corresponding efficiencies based on the normal "ideal" slope of  $2\pi$  are 80 and 102% respectively.

To account for the change in the angle of zero lift requires a consideration of the superposed flow due to a sink. The theoretical lift due to a sink\*\* located  $x$  distance (measured in chord fractions) aft of the midpoint of a wing is independent of angle of attack and is given by

$$\Delta C_L = 2C_Q \frac{\sqrt{1-4x^2}}{1-2x}$$

For slot  $G_3$  ( $x = 20\%$ )  $\rightarrow \Delta C_L = 3.06 C_Q$ . Thus, at angles in the

\*  $C_{L0} = 2\pi (1 + .77 \frac{d}{t})$  where  $\frac{d}{t}$  = average thickness ratio = 18%;  $C_{L0} = 2\pi \cdot 1.14$

\*\* See appendix I

neighborhood of zero lift (where variations in slope of the lift curve will not distort the picture,) the increase in  $C_L$  should be linear with the increase in  $C_Q$ . The curves under examination show this to be approximately the case if consideration is not given the base run ( $C_Q = 0$ ) and only increments in  $C_Q$  accounted for. The relatively large increase in lift caused by the first application of suction may be explained as follows:

With no suction, the rear stagnation point of the airfoil is not at the trailing edge but, because of the thick boundary layer existing at the rear of the section, is actually some distance in front of it on the upper surface of the wing. The first action of suction is to move this stagnation point aft a distance  $S$  (in % chord), thus, increasing the lift by

$$\Delta C_L = 0.4 \pi \sqrt{S} \quad *$$

If, as is the case in going from  $C_Q = 0$  to  $C_Q = .0063$ ,  $\Delta C_L = .045$ , at  $\alpha = -2^\circ$ , then  $S = 1.3 \times 10^5\%$ , a result which appears altogether reasonable.

The increase in lift coefficient (for WBGz from 1.20 to 2.10, for WBGzF from 2.13 to 2.80) is thus accomplished, for the most part, by an approach to perfect fluid flow, as evinced by the movement of the rear stagnation point toward the trailing edge and the increase of circulation for a given angle of attack; a minor effect is produced by the superposition of the flow due to a sink.

\* See appendix I

## 2. MOMENTS

The same mechanism should also account for any changes in wing pitching moment, and a consideration of Figures 4, 10, 13, in the light of an analysis similar to the preceding one shows this to be the case. A study of Figure 13 shows that the application of suction has increased the stability of the configuration by 5.5%. At the same time, it appears that the instability of the wing alone about the quarter chord point of the M. A. C. is 6%, thus placing its aerodynamic center at the 19% chord point. This a.c. seems rather far forward when compared with ordinary experimental results in the neighborhood of 23 to 24% for wings with no sweepback, but it does not appear unlikely in view of the generally bad characteristics of the wing alone as indicated by a "normal" wing efficiency of but 80%. Eliminating the de-stabilizing effect of the fuselage, the effect of suction on stability corresponds to a shift in a.c. from 19 to 24.5%. This increase in stability is the direct result of the decrease in boundary layer thickness and the resulting approach to perfect fluid flow, the a.c. for an airfoil in an ideal fluid being, of course, at the 25% point of the M. A. C.

To account for the shift in moment at zero lift, the moment due to a movement of the rear stagnation point as well as the moment due to a sink should be examined. If we consider the two configuration WBG<sub>3</sub> and WBG<sub>4</sub> (G<sub>3</sub> taped), the theoretical

lifts and moments due to a sink for the two cases are:

WBG <sub>3</sub>	WBG <sub>4</sub>
$C_L = 3.06 C_Q$	$C_L = 1.74 C_Q$
$C_{M.25} = 1.22 C_Q$	$C_{M.25} = 1.30 C_Q$

If, now, we assign any experimental increase in lift, greater than the above values, to a shift in the rear stagnation point and calculate the effect of such a shift on the moment at zero lift, then add to this the moment due to the sink, we can hope for reasonable correlation with the observed data. The moment, about the 25% point, due to a shift in the rear stagnation point which gives a lift increase,  $C_{LS}$ , is  $C_{MS} = -\frac{C_{LS}^*}{4}$

Tabulating for the two cases from Figures 10 and 13.

WBG<sub>3</sub>      q = 7

$C_Q$	$C_{L_{exp.}}$	$3.06C_Q$	$C_{LS}$	$C_{MS}$	$1.22 C_Q$	$C_M$ calc.	$C_{M_{exp.}}$
.0187	.085	.058	.027	-.0067	.0230	.0163	-.0040
.0125	.065	.038	.027	-.0067	.0152	.0085	-.0070
.0063	.045	.018	.027	-.0067	.0077	.0010	-.0100

WBG<sub>4</sub>      q = 7

$C_Q$	$C_{L_{exp.}}$	$1.74 C_Q$	$C_{LS}$	$C_{MS}$	$1.30C_Q$	$C_M$ calc.	$C_{M_{exp.}}$
.018	.062	.032	.030	-.0075	.0234	.0159	.0150
.012	.043	.020	.023	-.0057	.0156	.0099	.0100
.006	.032	.010	.022	-.0055	.0078	.0023	.0045

Comparing the last two columns in each table shows that, while the actual magnitude of the calculated  $C_M$ 's does not in both cases agree too closely with observed values, the differences in going from one  $C_Q$  to another are quite comparable and altogether within experimental accuracy. It appears, thus, that the foregoing analysis

\* See Appendix I

provides a suitable explanation for the magnitude and direction of the changes that occur in the lift and moment curves.

### 3. DRAG

A consideration of the drag curves, Figures 14-19, shows that the so-called "ideal parasite drag" decreases with increasing  $C_Q$ . This result is to be expected in view of the decreased boundary layer thickness, and the resulting decrease in skin friction, associated with an increase in suction. The equivalent parasite drag (i.e.  $CD_p + CD_s$ ) is, however, in every case increased with suction, although Figure 24 indicates the possibility of a minimum occurring at some high Reynolds Number.

### 4. EFFECT OF SLOT LOCATION

Figures 12, 19, 20, showing the effect of slot location on three-component and parasite drag data, clearly indicate the superiority of the single slot  $G_3$  over slot  $G_4$  or any combinations of slot  $G_3$  and  $G_4$ . Not only is this slot superior in the effect produced by a given amount of suction, but, as indicated by Figure 21, requires less power for a given quantity of air removed.

### 5. SCALE EFFECT

The majority of the runs made in this particular series of tests were made with the purpose in mind of finding the variation of the effects of suction with Reynolds Number. It appears, from the results obtained, that a given effect can be accomplished at a high Reynolds Number with a lower expenditure of power than at a low Reynolds Number.

Consider Figure 22 showing the variation of the increment in maximum lift coefficient with  $C_Q$  for various Reynolds Numbers. The individual curves have the characteristic shape of all such plots, the curve for a  $q$  of 7 indicating the limit of useful  $C_Q$ 's has already been reached. The significant feature of the family is the shift to the right of curves of the lower Reynolds Numbers, indicating that a given effect requires increased suction for decreasing Reynolds Numbers. A cross-plot of this curve, shown in Figure 23, indicates more specifically this variation. As can be seen, there is a very considerable scale effect which is, however, questionable in the range of Reynolds Numbers technically important. The family indicates that, for a given lift increment, the required quantity of air removed and hence the power required (see Figure 21) drop steadily with increasing Reynolds Number, in the range tested. Extending these results to any Reynolds Number beyond test values is very questionable and little if any attention should be paid to the dotted extensions of the solid line.

The same procedure was followed in an attempt to determine the scale effect on the "ideal" parasite drag coefficient  $C_{Dp}'$  with much the same results. It was found that the available data indicated a very sharp decrease in power required to affect a given percentage decrease in drag with increasing Reynolds Number. Unfortunately, the drag data obtained was rather meager and, further, was entirely disqualified for any Reynolds Number extrapolations by the discovery that the wing was in the transition region, as shown in Figure 25.

This lack of any reasonable Reynolds Number extrapolation of drag results makes the problem of evaluating the possible utility of suction in flight rather indeterminate, since any conclusions will vary greatly with the assumption made as to the power required to produce a given effect. The question of performance with suction is thus left waiting for want of more reliable drag data. It is the expectation of the authors to obtain such data very shortly by inducing artificial turbulence in the wind tunnel\*, thus avoiding the transition region which is so troublesome.

\* See Appendix II

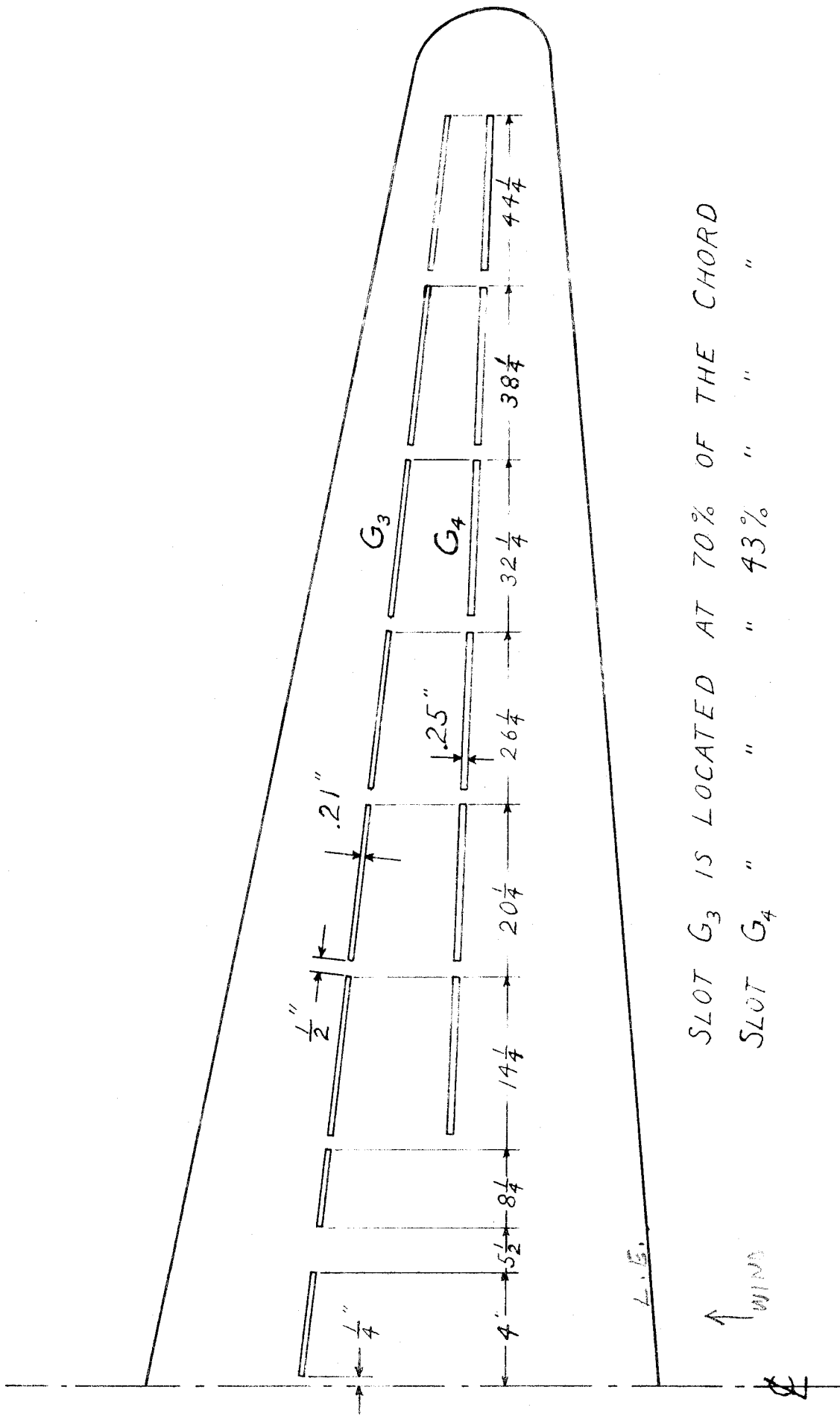


## REFERENCES

1. Smith, A. M. O., A Preliminary Study of the Problem of Boundary Layer Control. C. I. T. Master Thesis, 1938
2. Bowen, W. H., Tests on Axial Flow Fans Designed by Lattice Theory. C. I. T. Master Thesis, 1938
3. Ackeret, J., Betz, A., Schrenk, O., Experiments with an Airfoil from which the Boundary Layer is Removed by Suction. NACA Technical Memorandum 374
4. Schrenk, O., Experiments with a Sphere from which the Boundary Layer is Removed by Suction. NACA Technical Memorandum 388
5. Ackeret, J., Removing Boundary Layer by Suction. NACA Technical Memorandum 395
6. Seewald, F., Increasing Lift by Releasing Compressed Air on Suction Side of Airfoil. NACA Technical Memorandum 441
7. Reed, E. G., Bamber, M. J., Preliminary Investigation on Boundary Layer Control by Means of Suction and Pressure with the U. S. A. 27 Airfoil. NACA Technical Note 286
8. Knight, M., Bamber, M. J., Wind Tunnel Tests on Airfoil Boundary Layer Control Using a Backward Opening Slot. NACA Technical Note 323
9. Schrenk, O., Experiments with a Wing Model from which the Boundary Layer is Removed by Suction. NACA Technical Memorandum 534
10. Schrenk, O., The Boundary Layer as a Means of Controlling the Flow of Liquids and Gases. NACA Technical Memorandum 555
11. Schrenk, O., Experiments with a Wing from which the Boundary Layer is Removed by Suction. NACA Technical Memorandum 634
12. Bamber, M. J., Wind Tunnel Tests on Airfoil Boundary Layer Control Using a Backward Opening Slot.
13. Schrenk, O., Experiments with Suction Type Wings. NACA Technical Memorandum 773

DIAGRAM SHOWING LOCATION OF SLOTS

FIG. 1  
34



SLOT G<sub>3</sub> IS LOCATED AT 70% OF THE CHORD  
 SLOT G<sub>4</sub> " " " 43% " " "

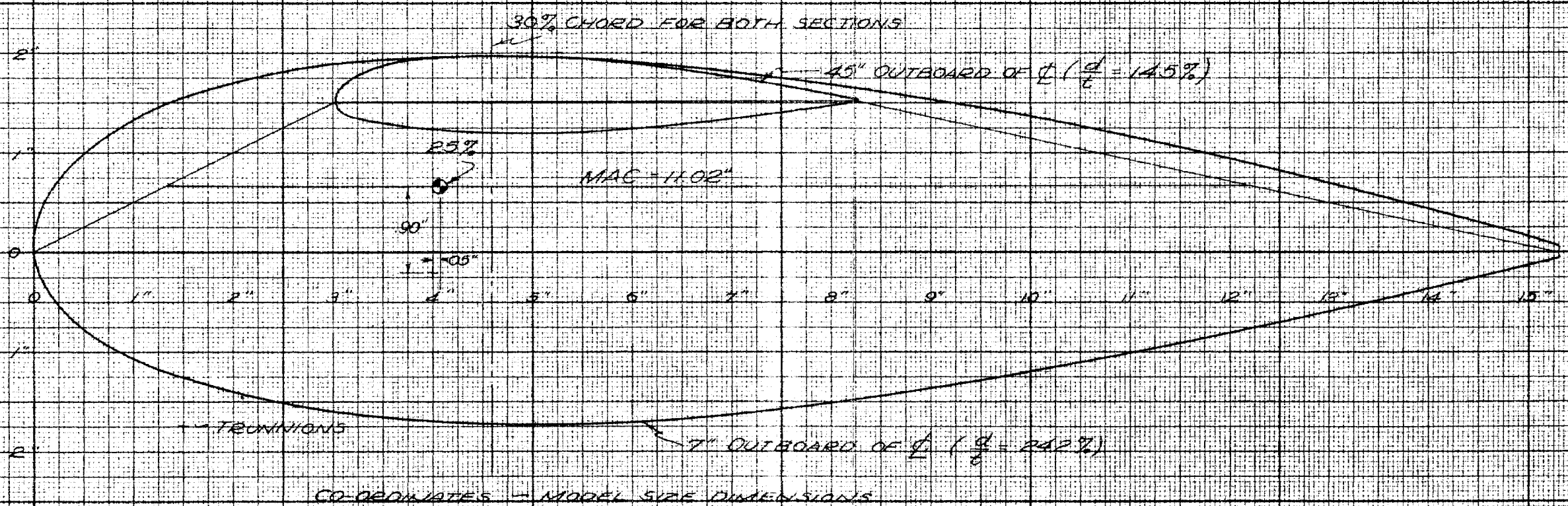
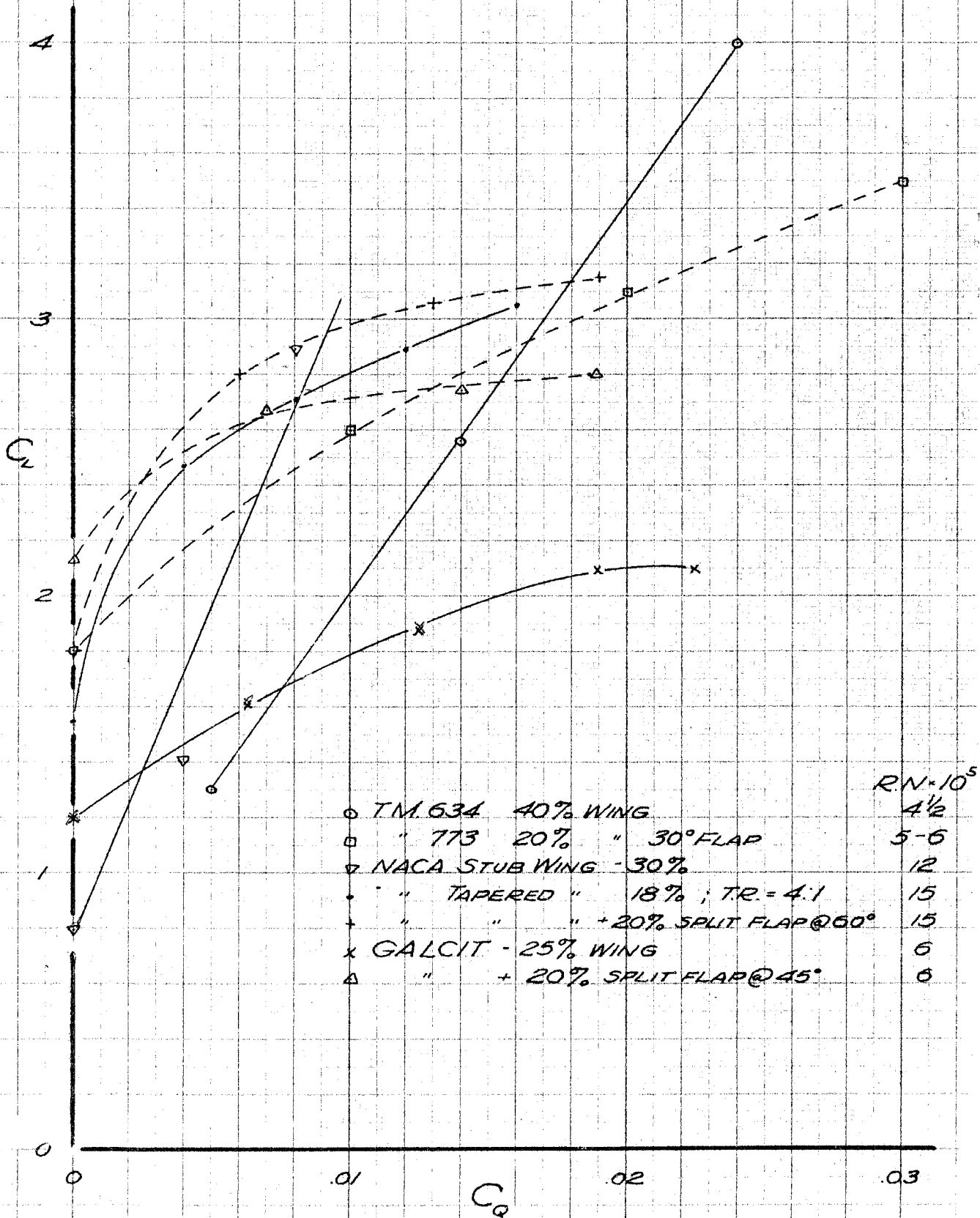
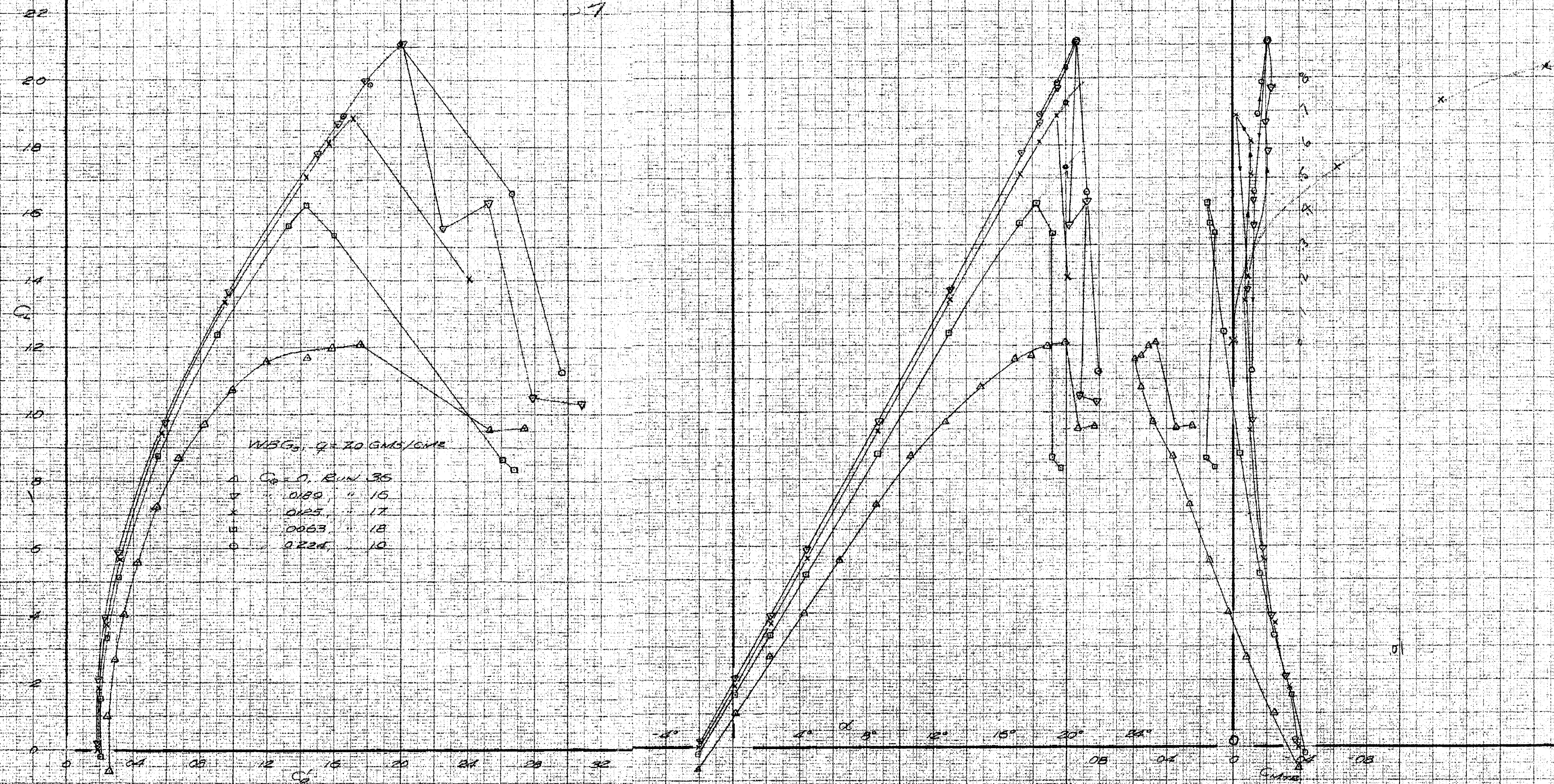


DIAGRAM SHOWING WING SECTIONS AND LOCATION OF MAC

36



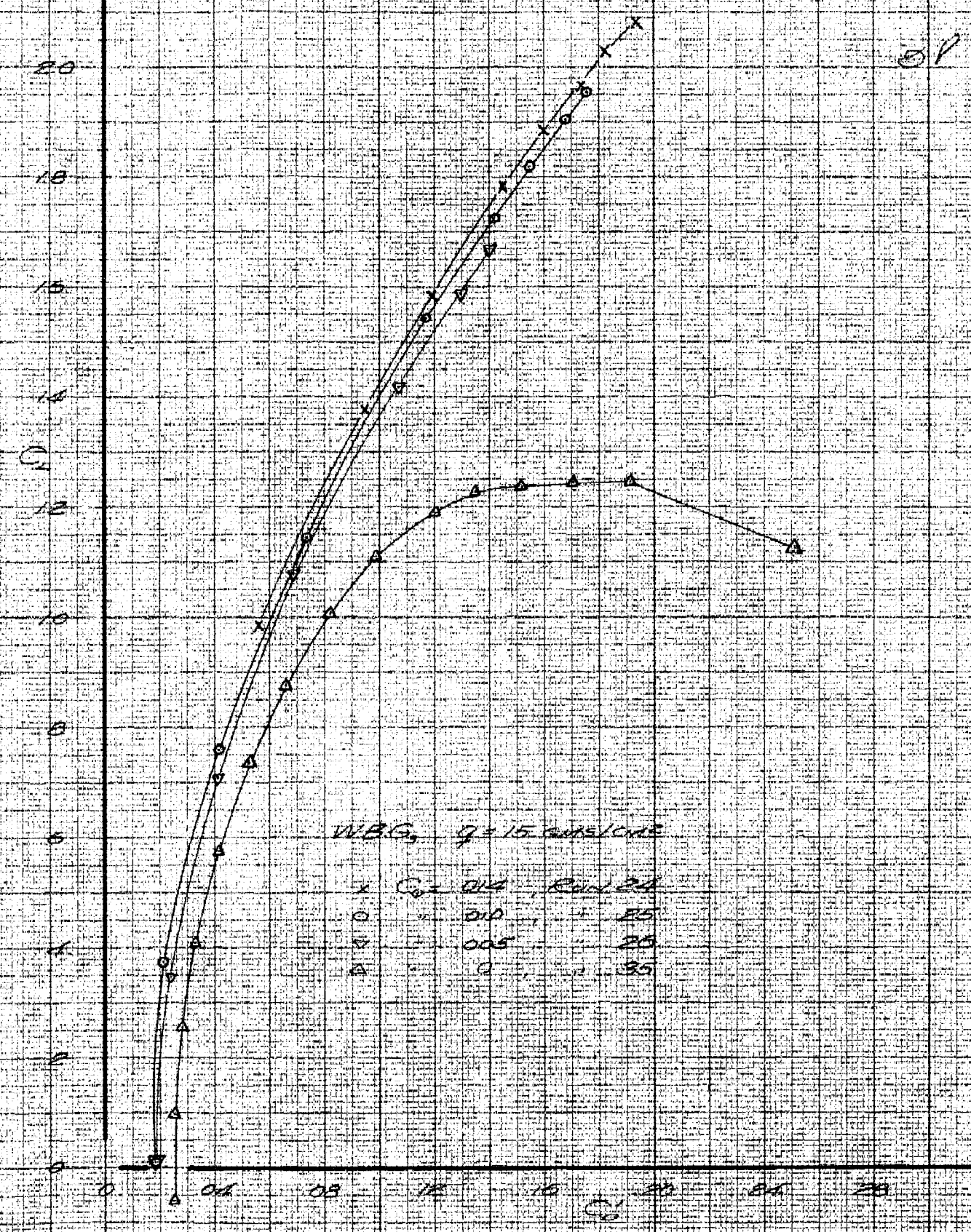
BEST RESULTS OF RECENT BOUNDARY  
LAYER REMOVAL EXPERIMENTS



EFFECT OF SYCTION ON THREE COMPONENT DATA

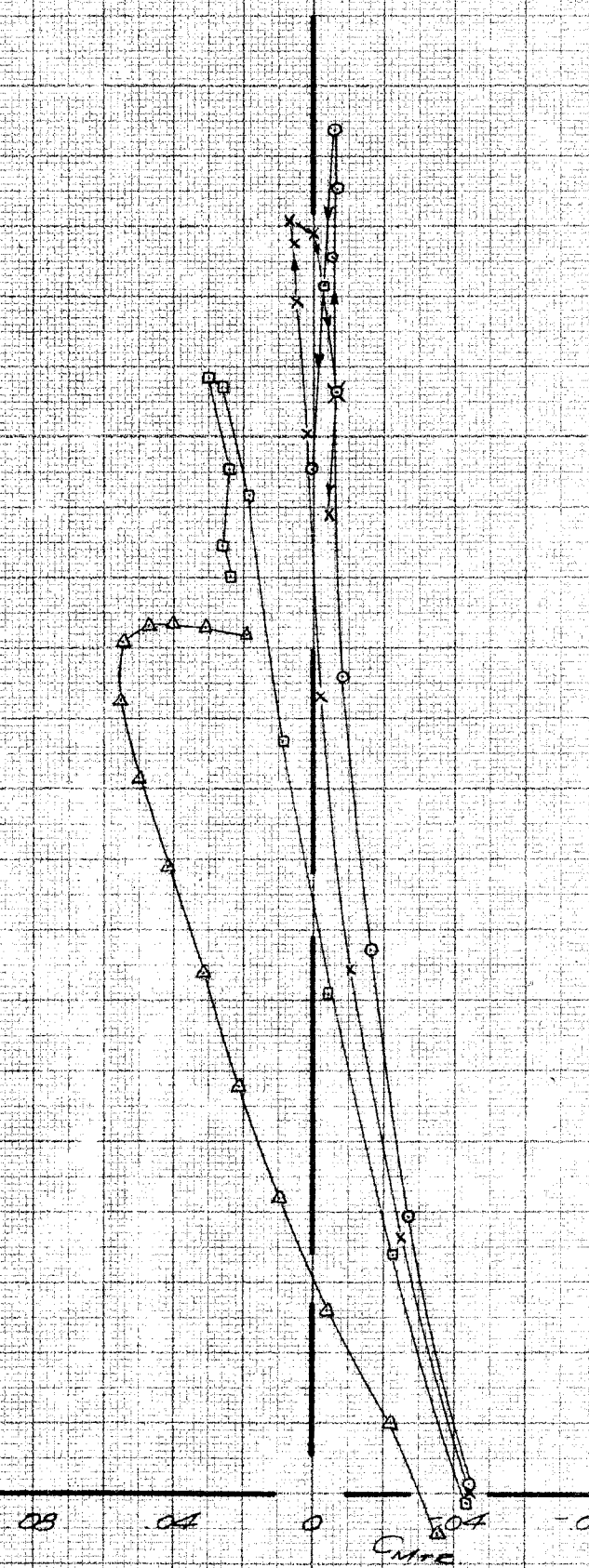
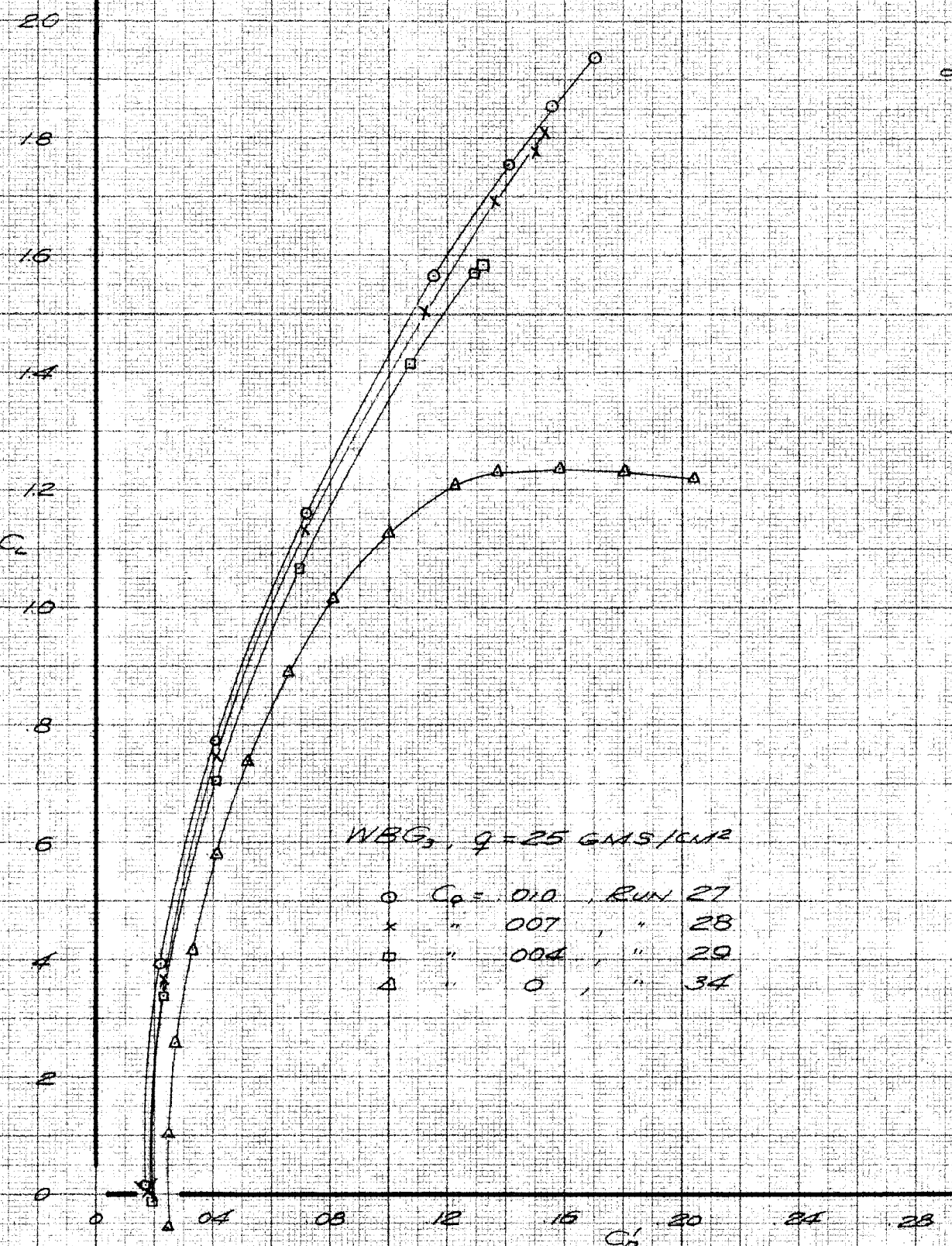
SLOP  $C_2$ ,  $q = 70$  GMS/CM<sup>2</sup>

51

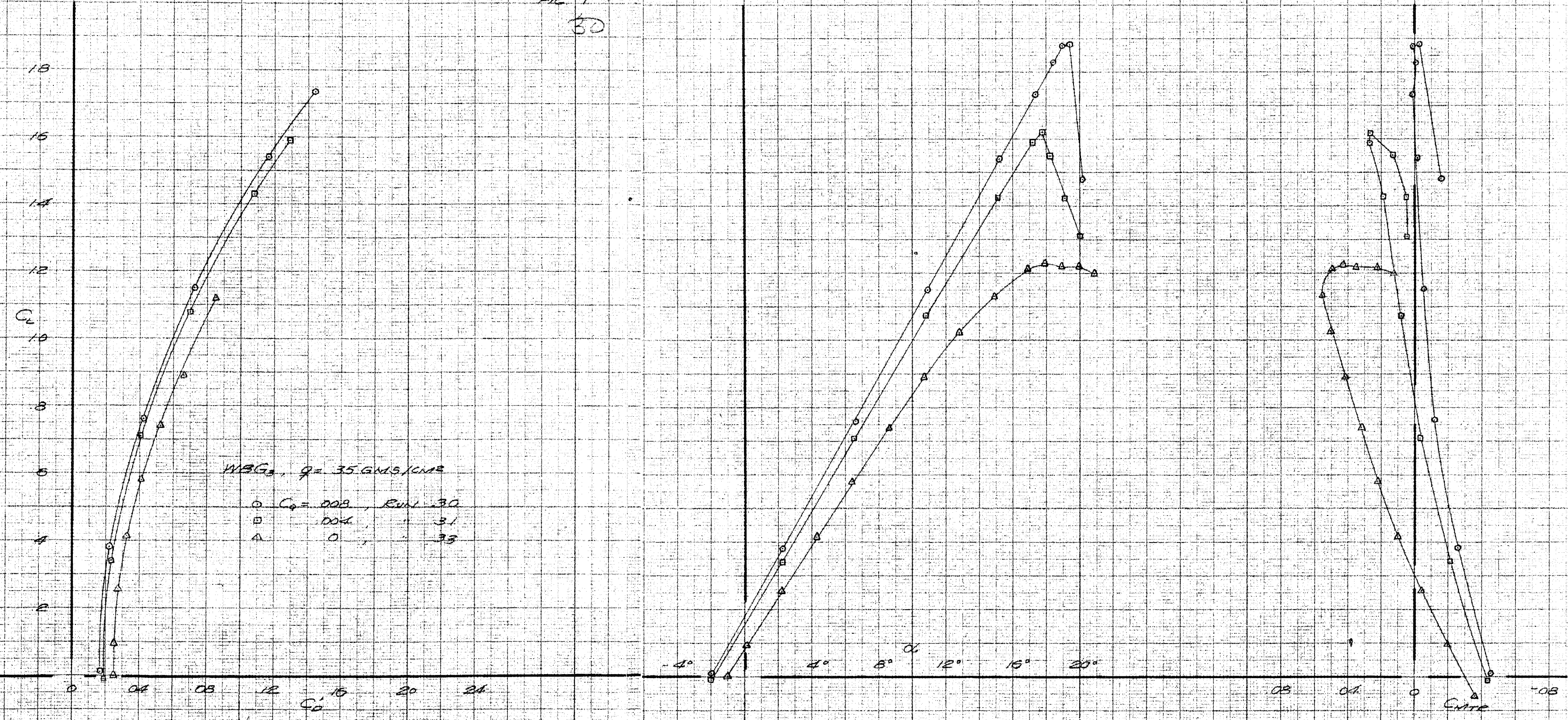


EFFECT OF SUCTION ON THREE COMPONENT DATA  
SLOT  $C_0$ ,  $q = 15$  GMS/CM<sup>2</sup>

29

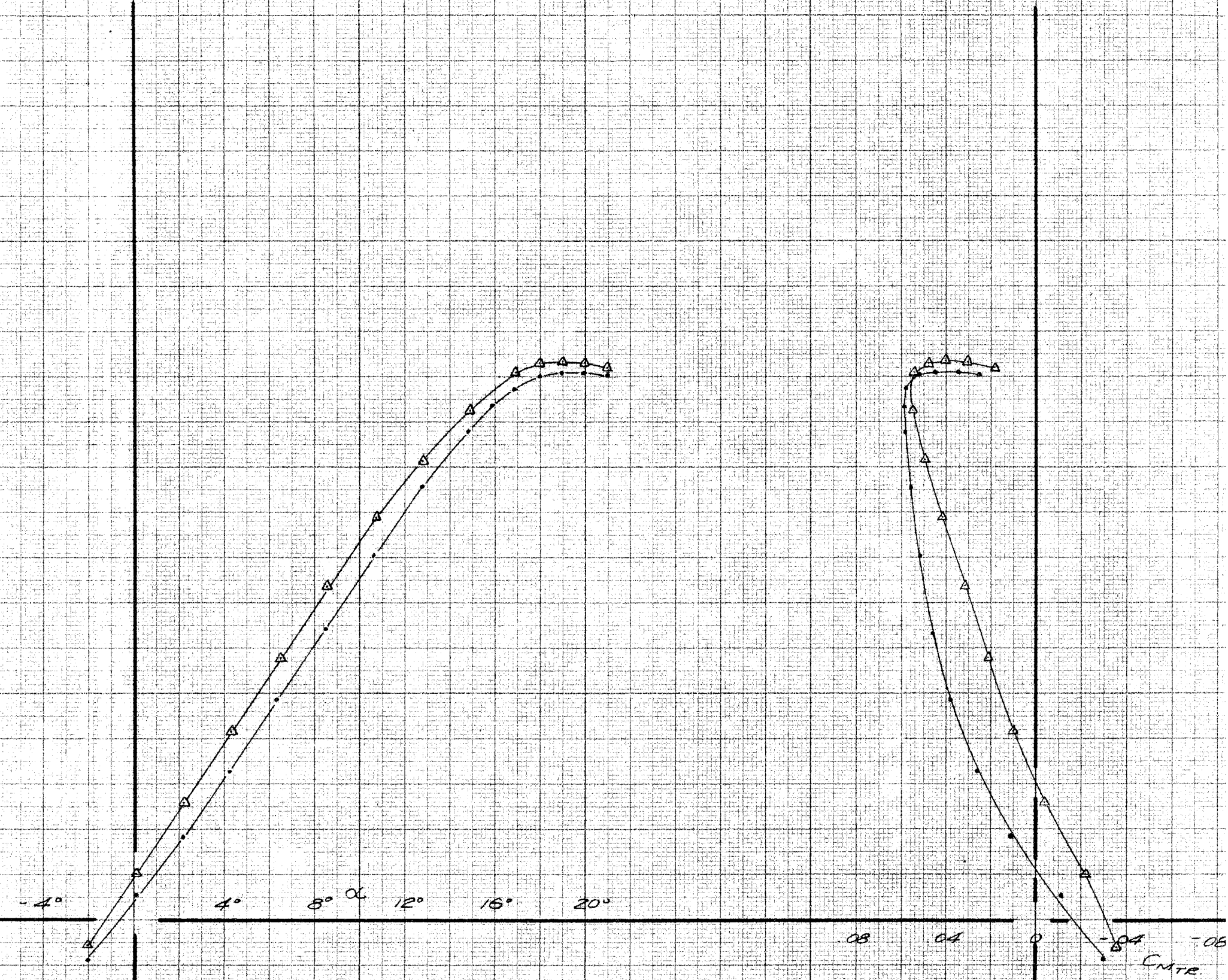
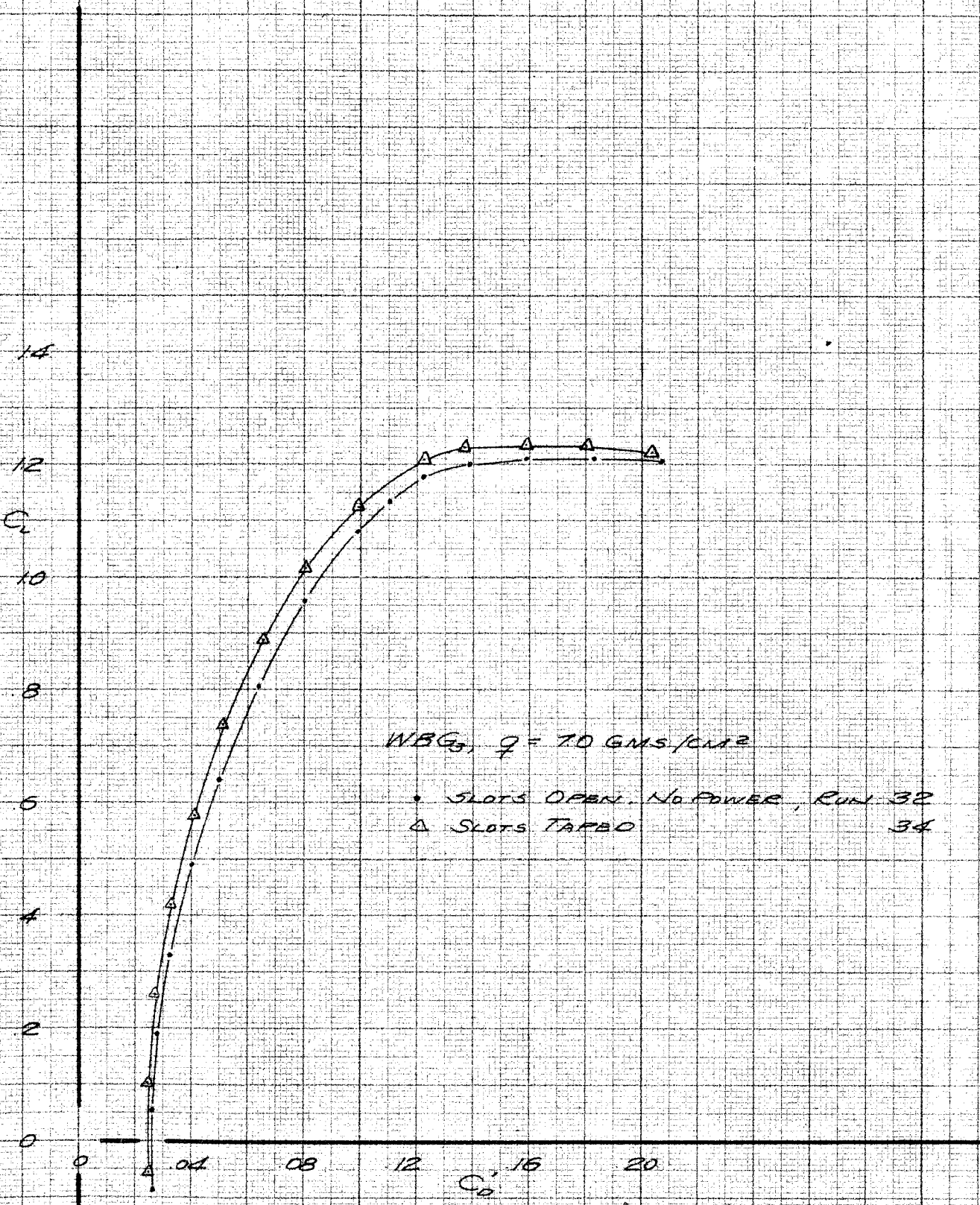


EFFECT OF SUCTION ON THREE COMPONENT DATA  
SLOT G<sub>3</sub>, q = 25 GMS/CM<sup>2</sup>

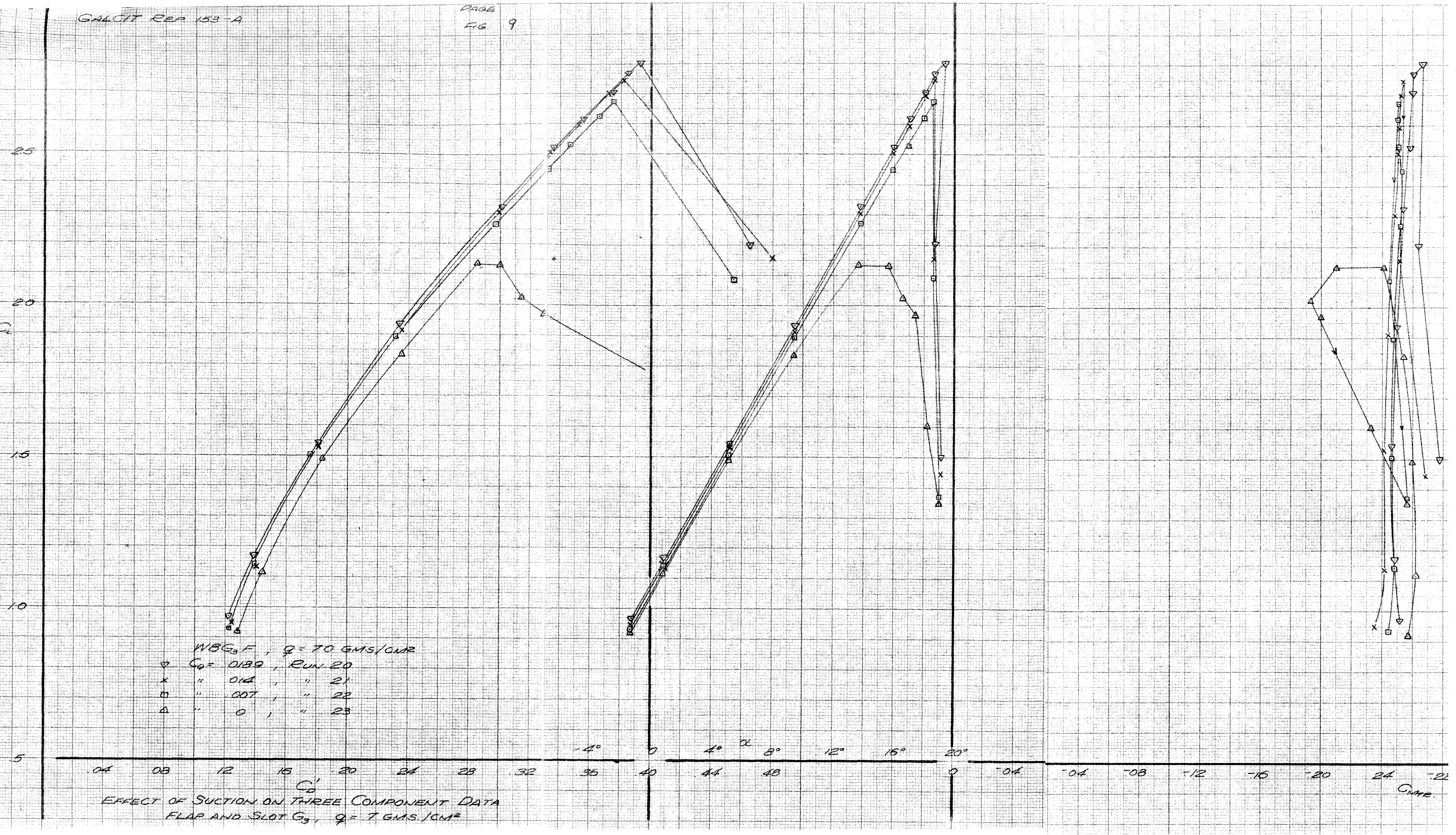


EFFECT OF SUCTION ON THREE COMPONENT DATA  
SLOT G<sub>3</sub>,  $Q = 35 \text{ GMS/CM}^2$



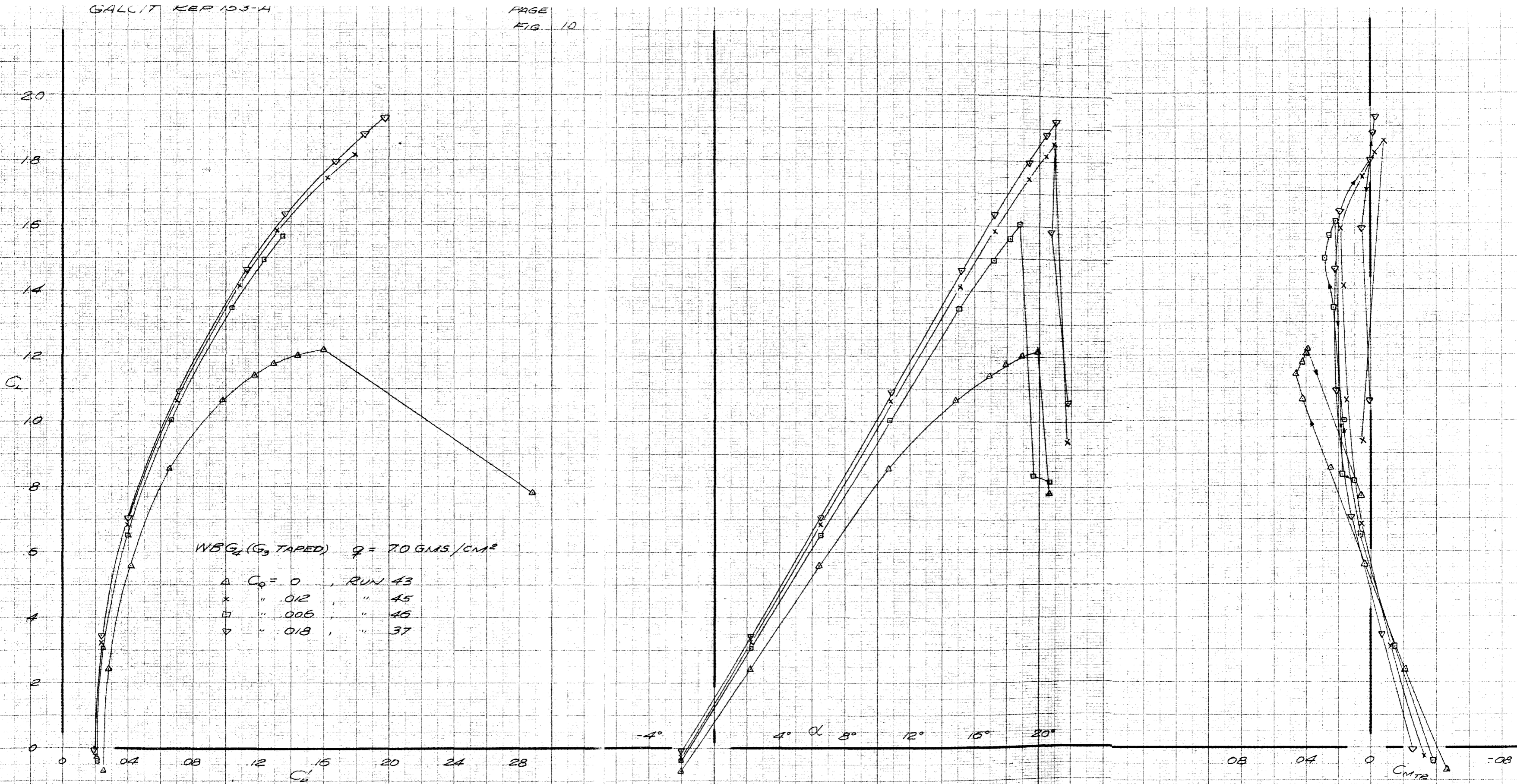


EFFECT OF TAPPING SLOT G<sub>3</sub> ON THREE COMPONENT DATA



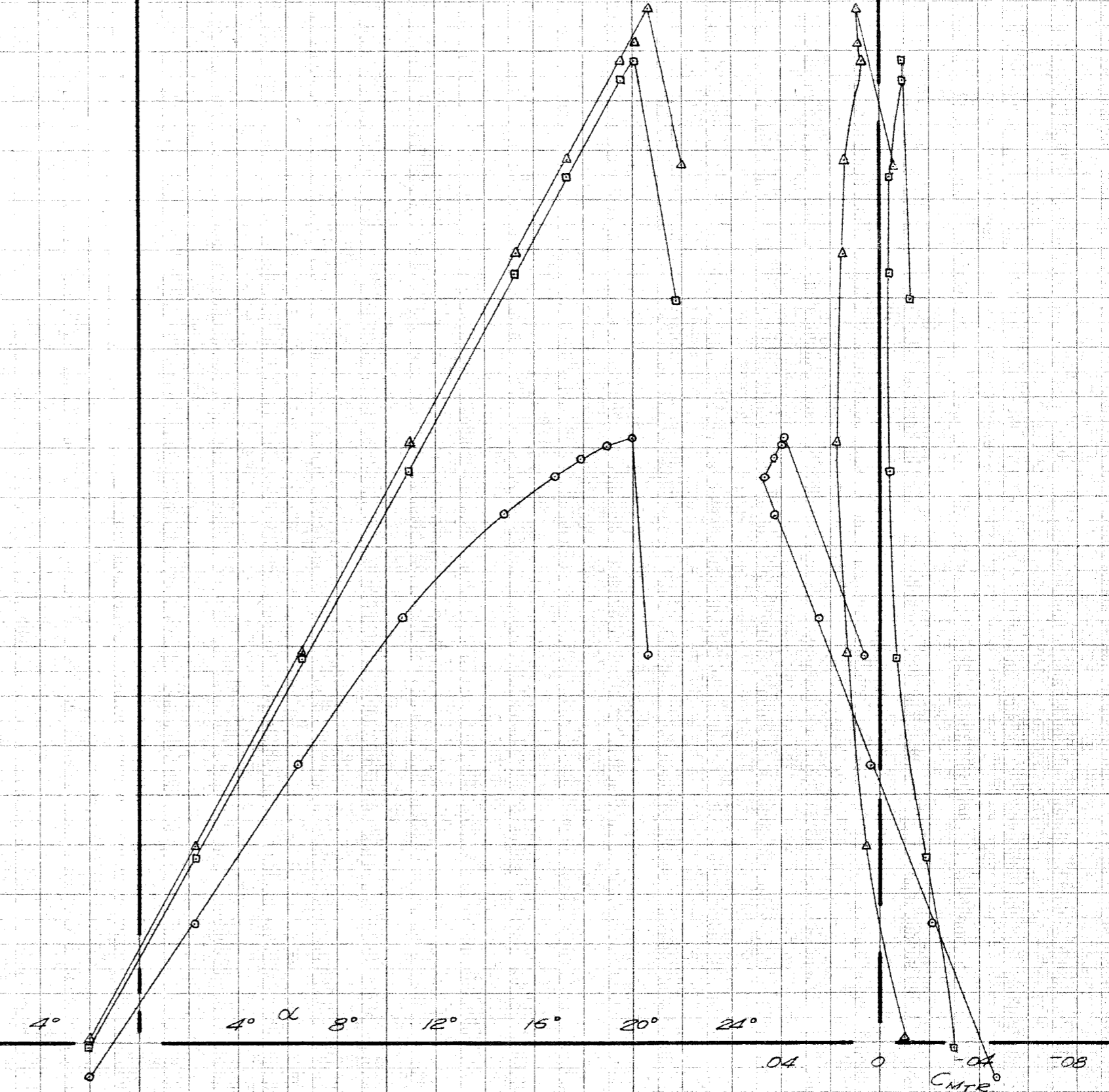
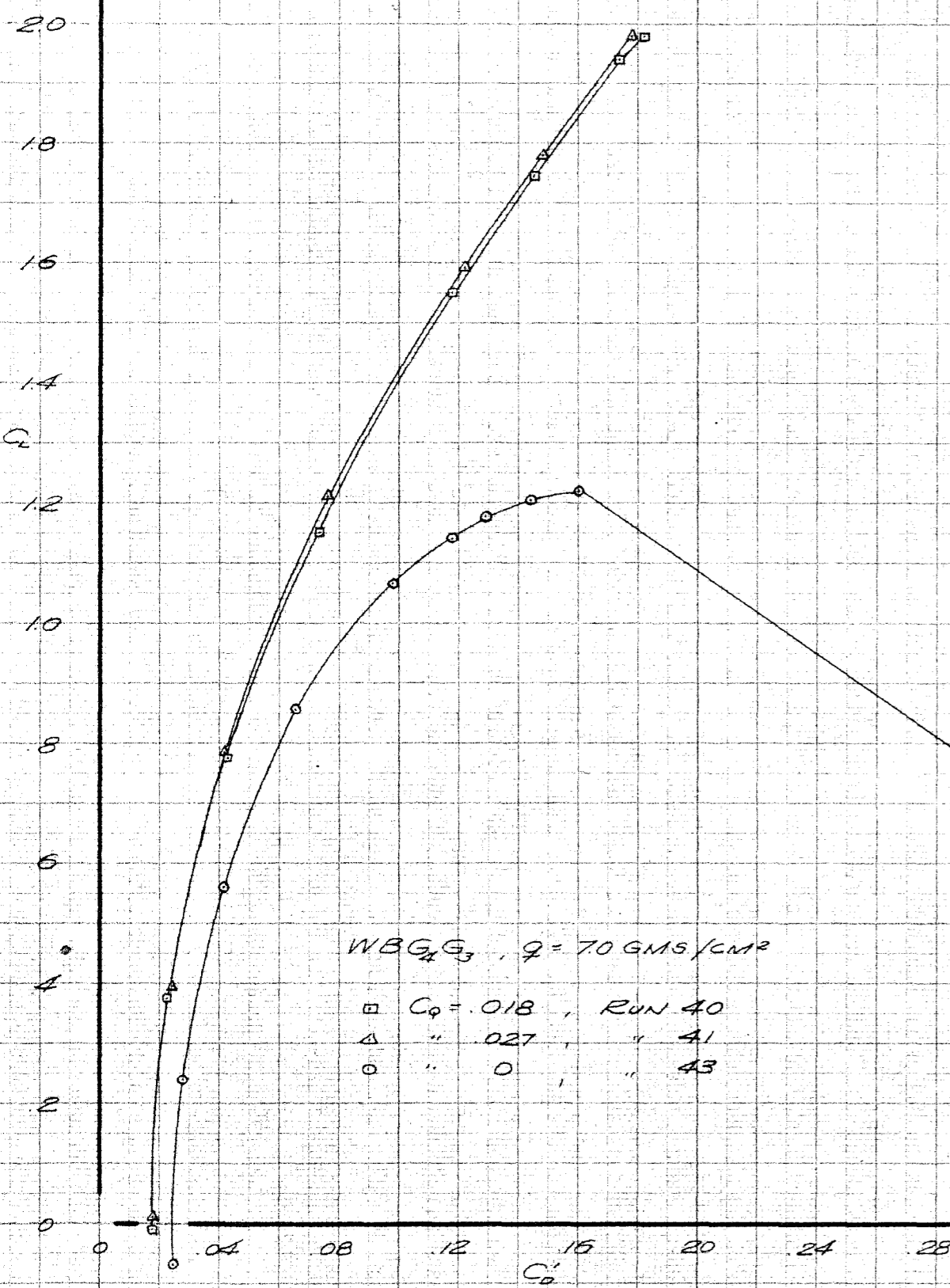
WBG<sub>3</sub>F,  $q = 70 \text{ GMS/CM}^2$   
 $\nabla$   $C_0 = 0.189$ , Run 20  
 $\times$  " 0.15, " 21  
 $\square$  " 0.07, " 22  
 $\triangle$  " 0, " 23

EFFECT OF SUCTION ON THREE COMPONENT DATA  
 FLAP AND SLOT  $G_3$ ,  $q = 7 \text{ GMS/CM}^2$

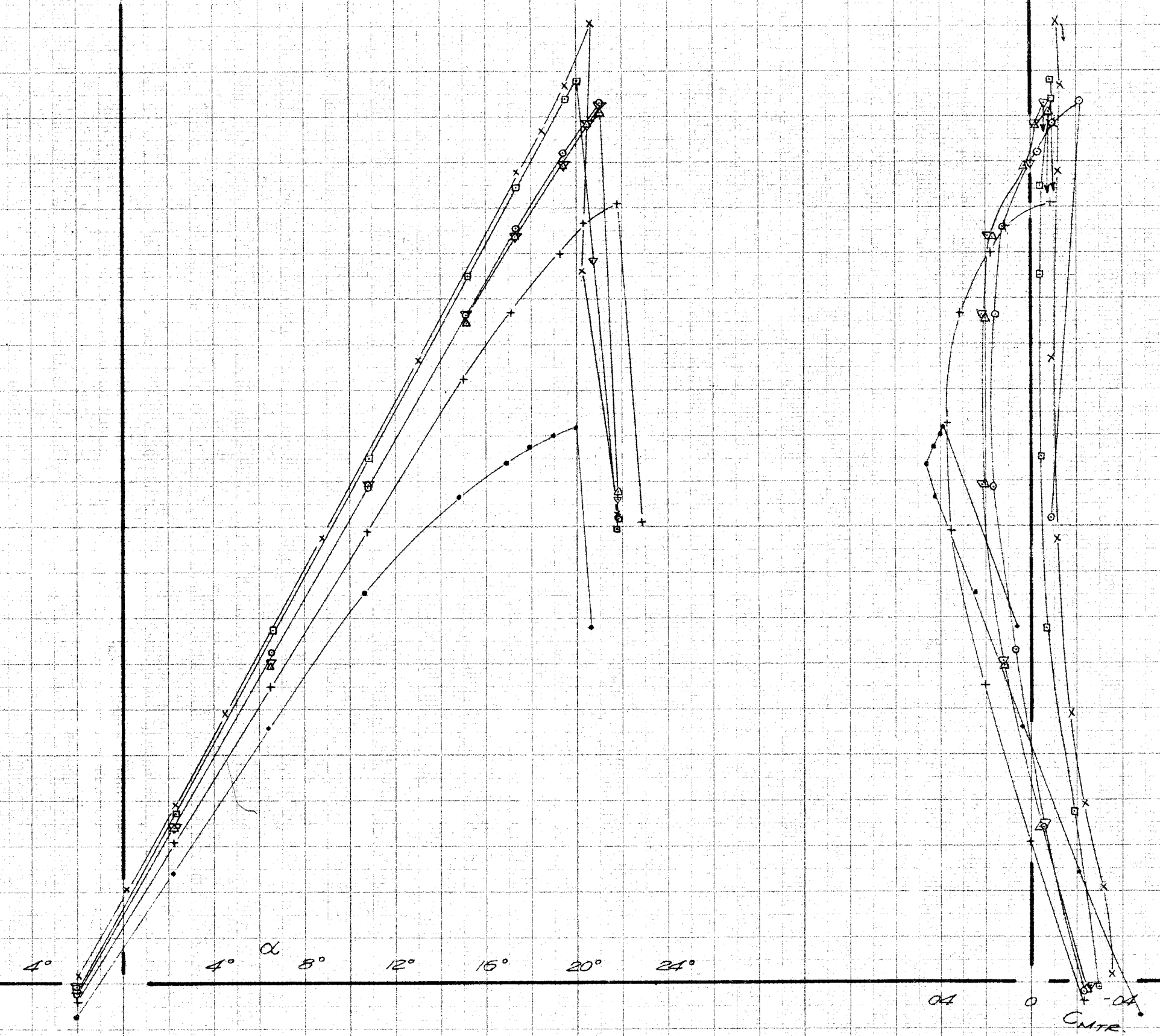
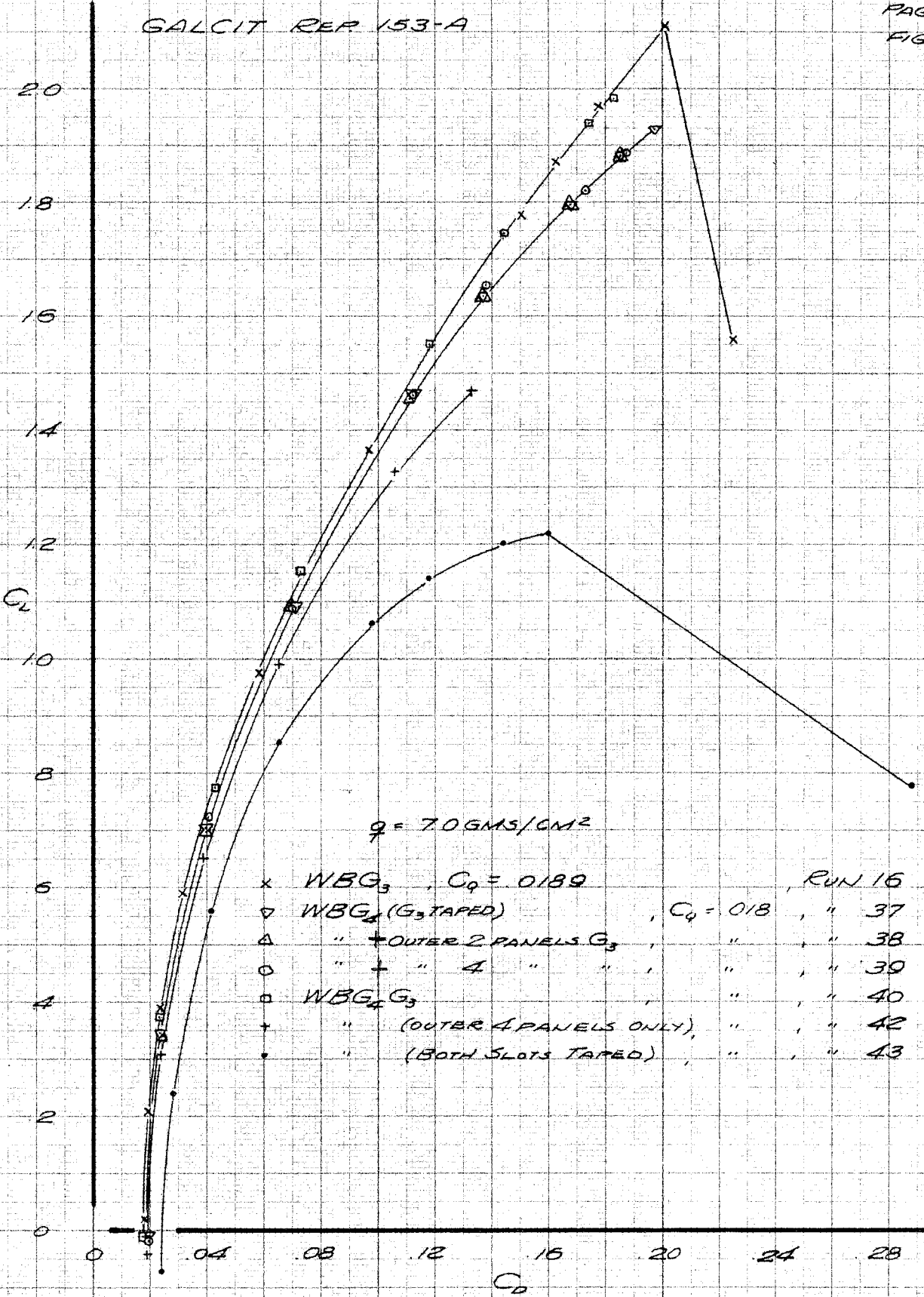


$WBG_4 (G_3 \text{ TAPED}) \quad q = 7.0 \text{ GMS/CM}^2$   
 $\Delta \quad C_s = 0, \text{ RUN } 43$   
 $\times \quad \text{" } 0.012, \text{ " } 45$   
 $\square \quad \text{" } 0.006, \text{ " } 46$   
 $\nabla \quad \text{" } 0.018, \text{ " } 37$

EFFECT OF SUCTION ON THREE COMPONENT DATA  
 SLOT  $G_4$ ,  $q = 7.0 \text{ GMS/CM}^2$

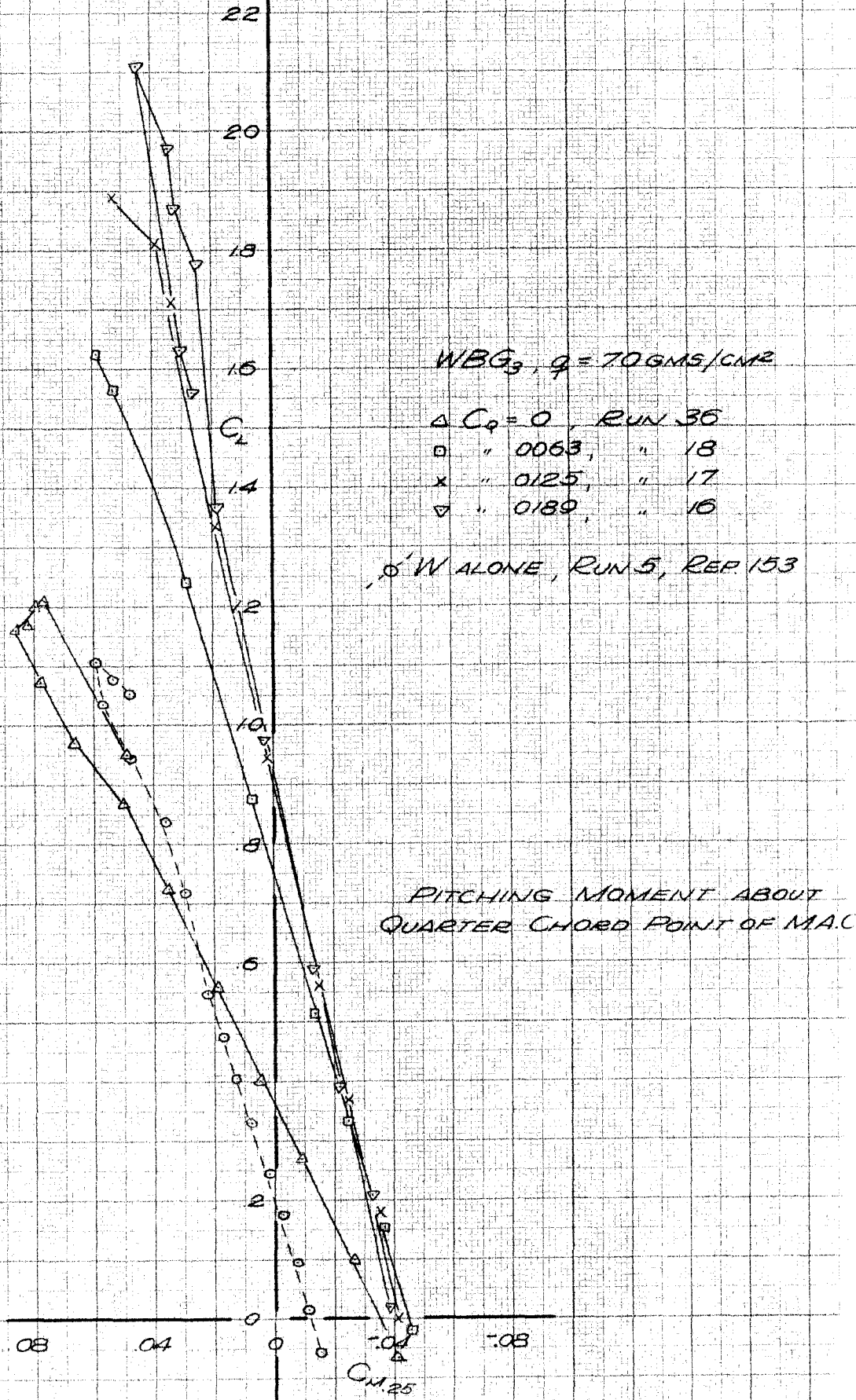


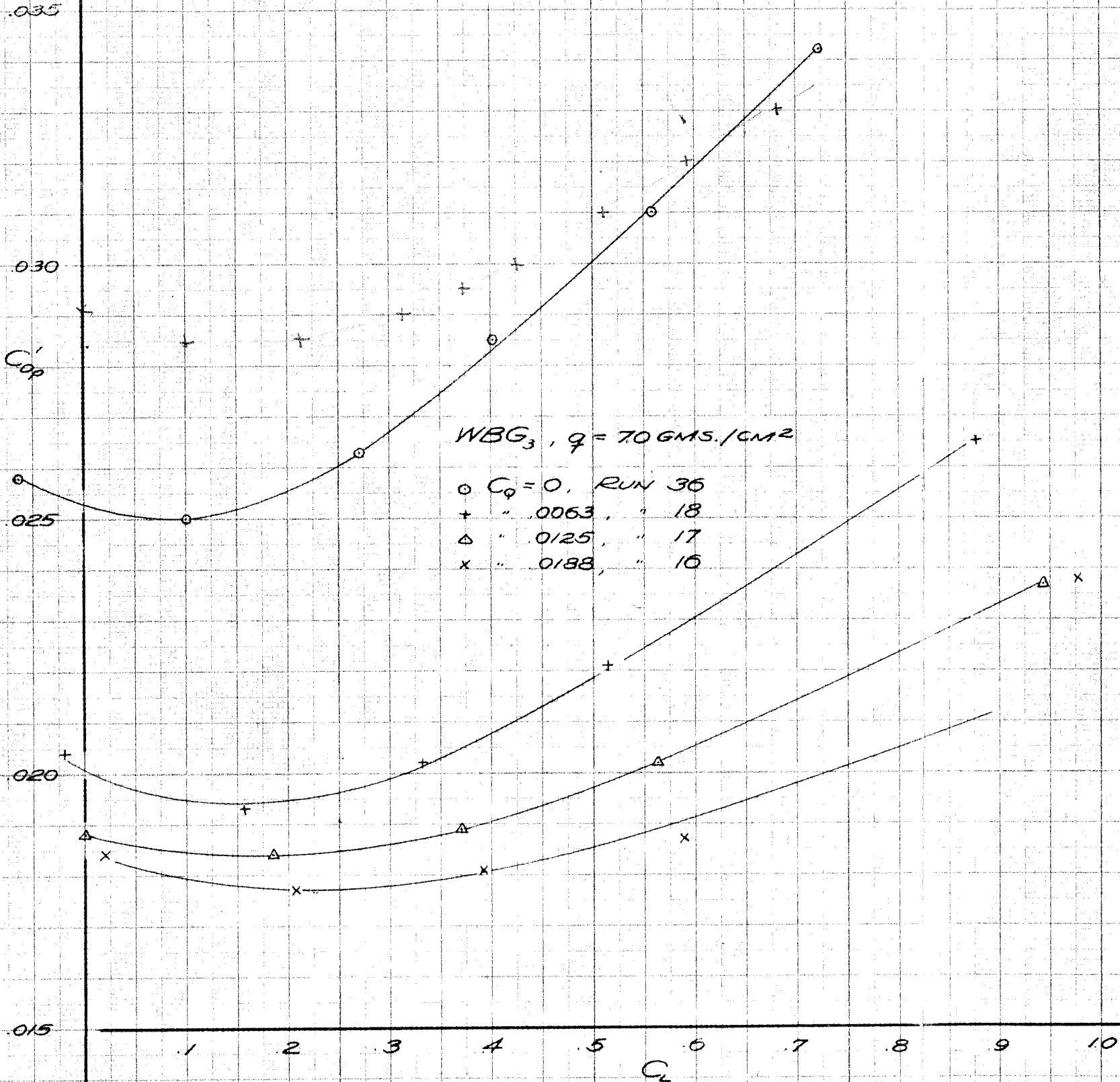
EFFECT OF SUCTION ON THREE COMPONENT DATA  
DOUBLE SLOTS,  $G_3, G_4$ ,  $q = 7 \text{ GMS/CM}^2$



EFFECT OF SLOT CONFIGURATION ON THREE COMPONENT DATA  
 $C_q = 0.18, q = 7 \text{ GMS/CM}^2$

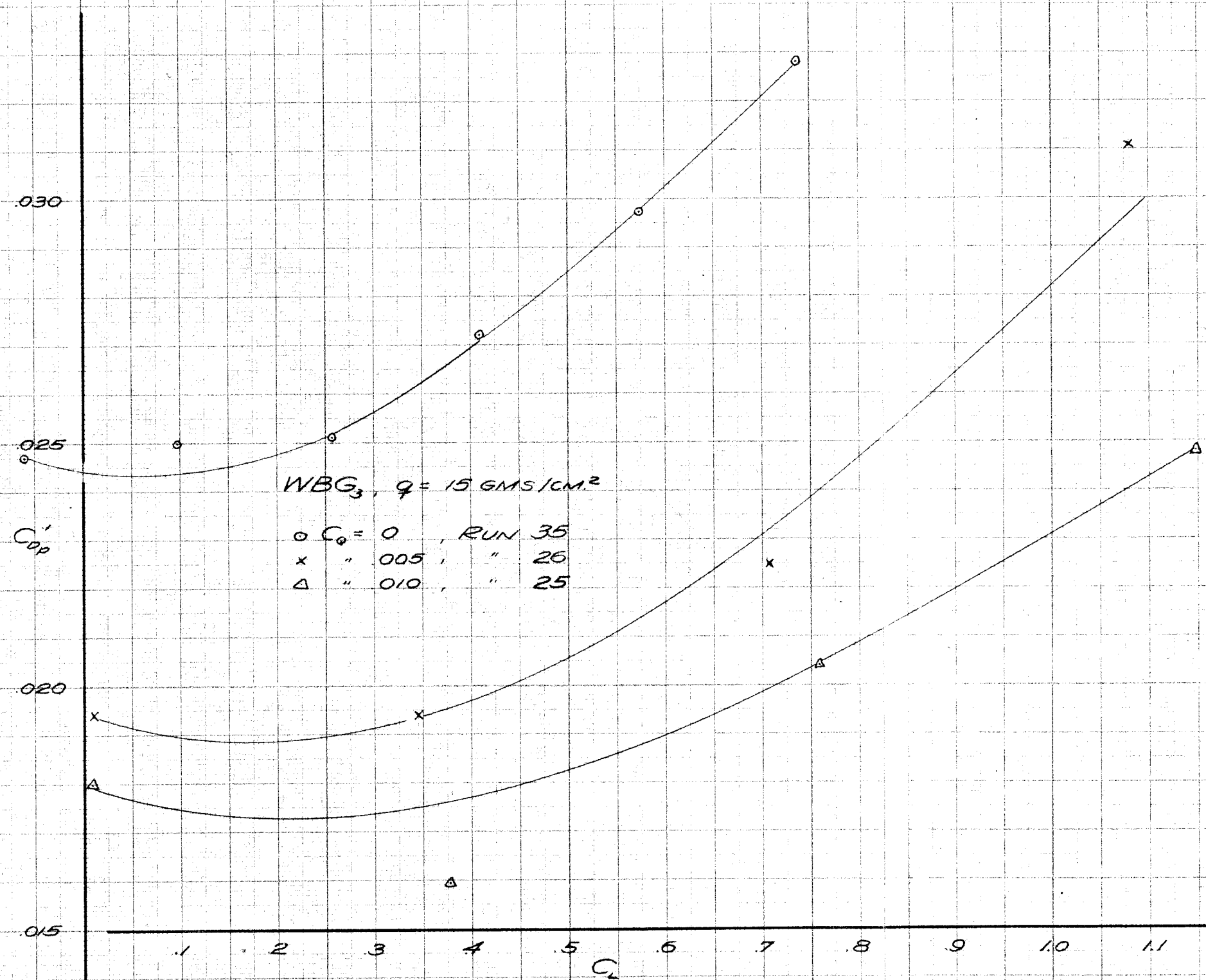
CNTRE





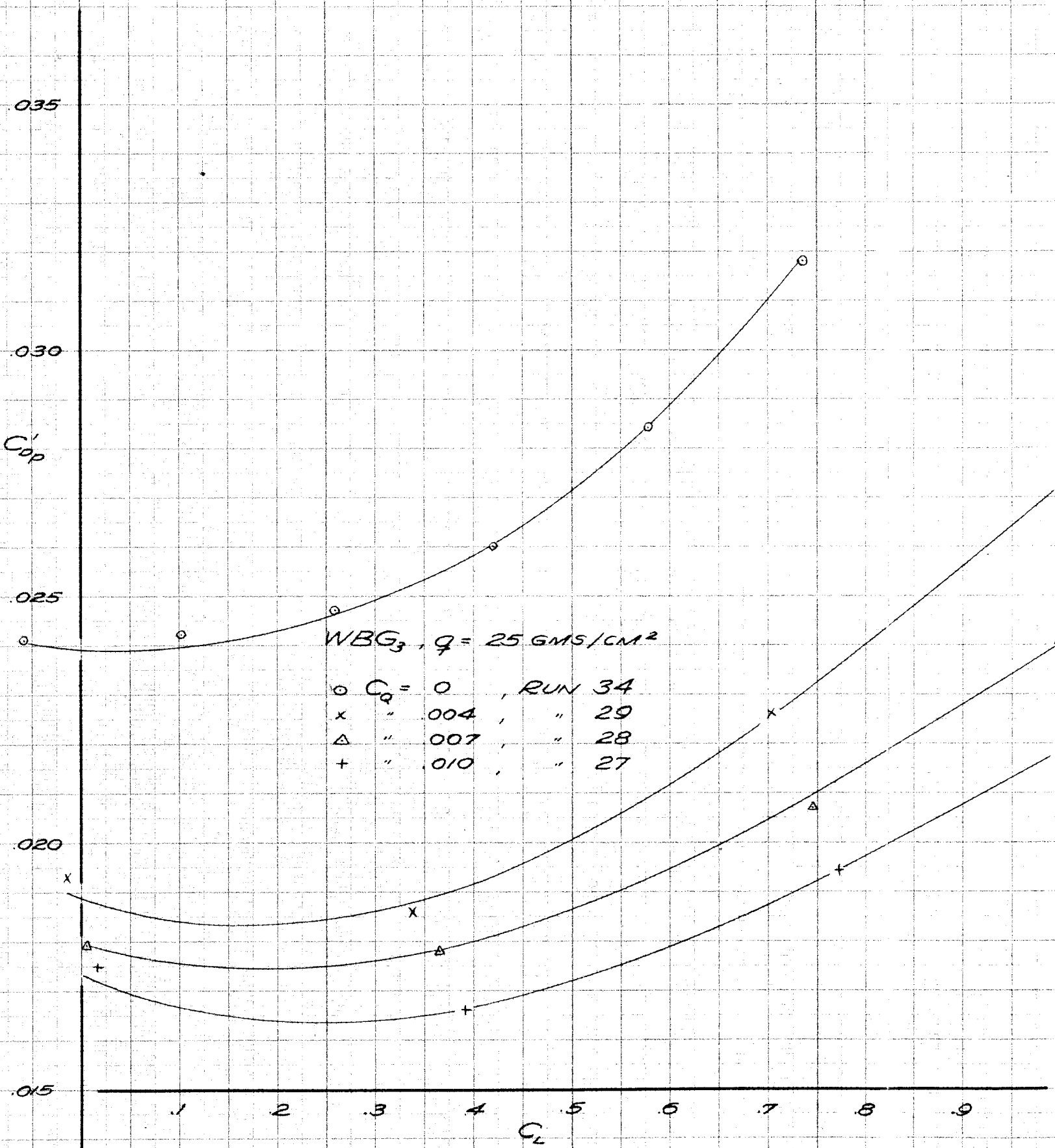
EFFECT OF SUCTION ON IDEAL PARASITE DRAG  
 $q = 7 \text{ GMS./CM}^2$

SLOT G<sub>3</sub>



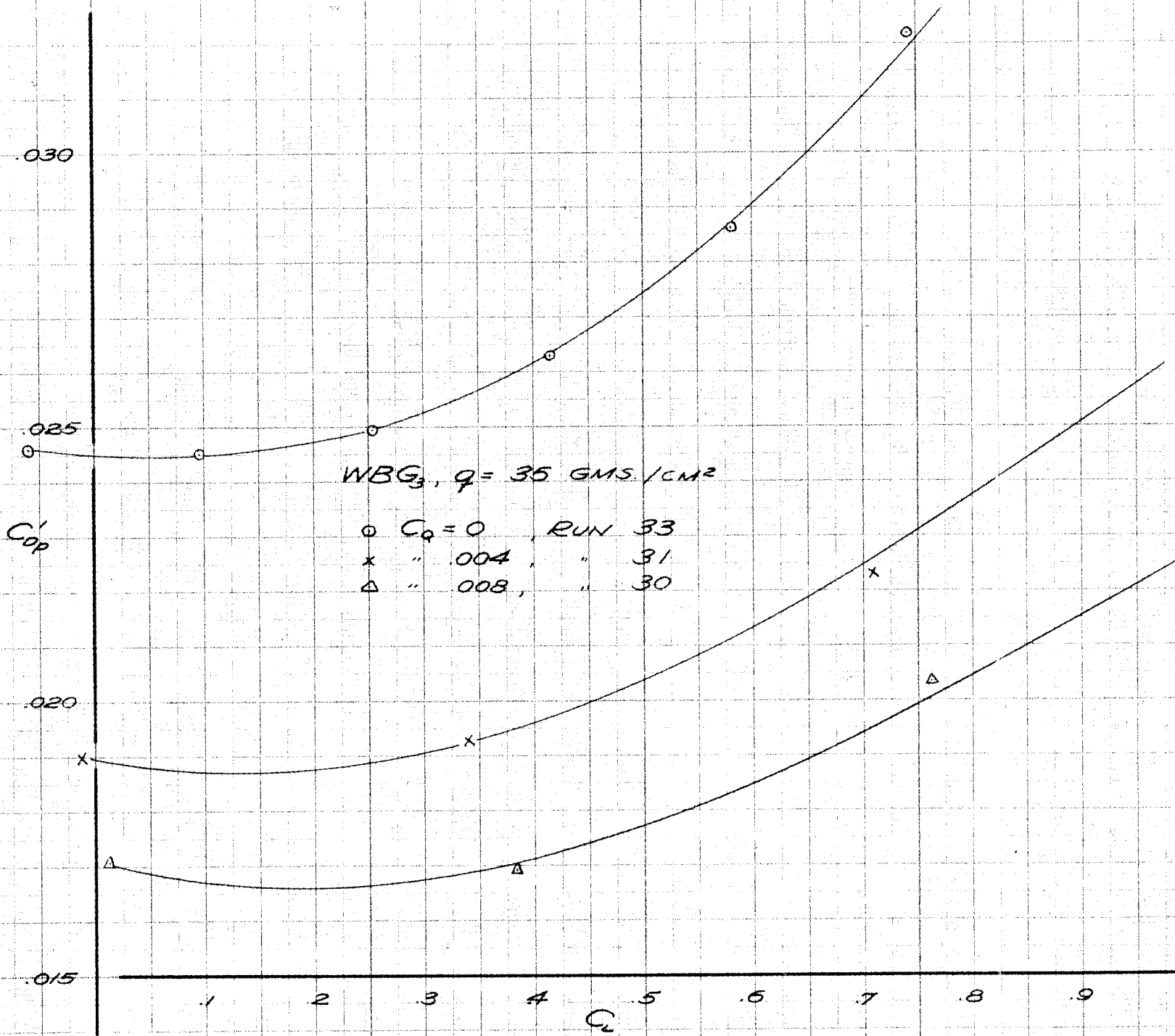
EFFECT OF SUCTION ON IDEAL PARASITE DRAG  
 $q = 15 \text{ GMS/CM}^2$   
 SLOT G<sub>3</sub>





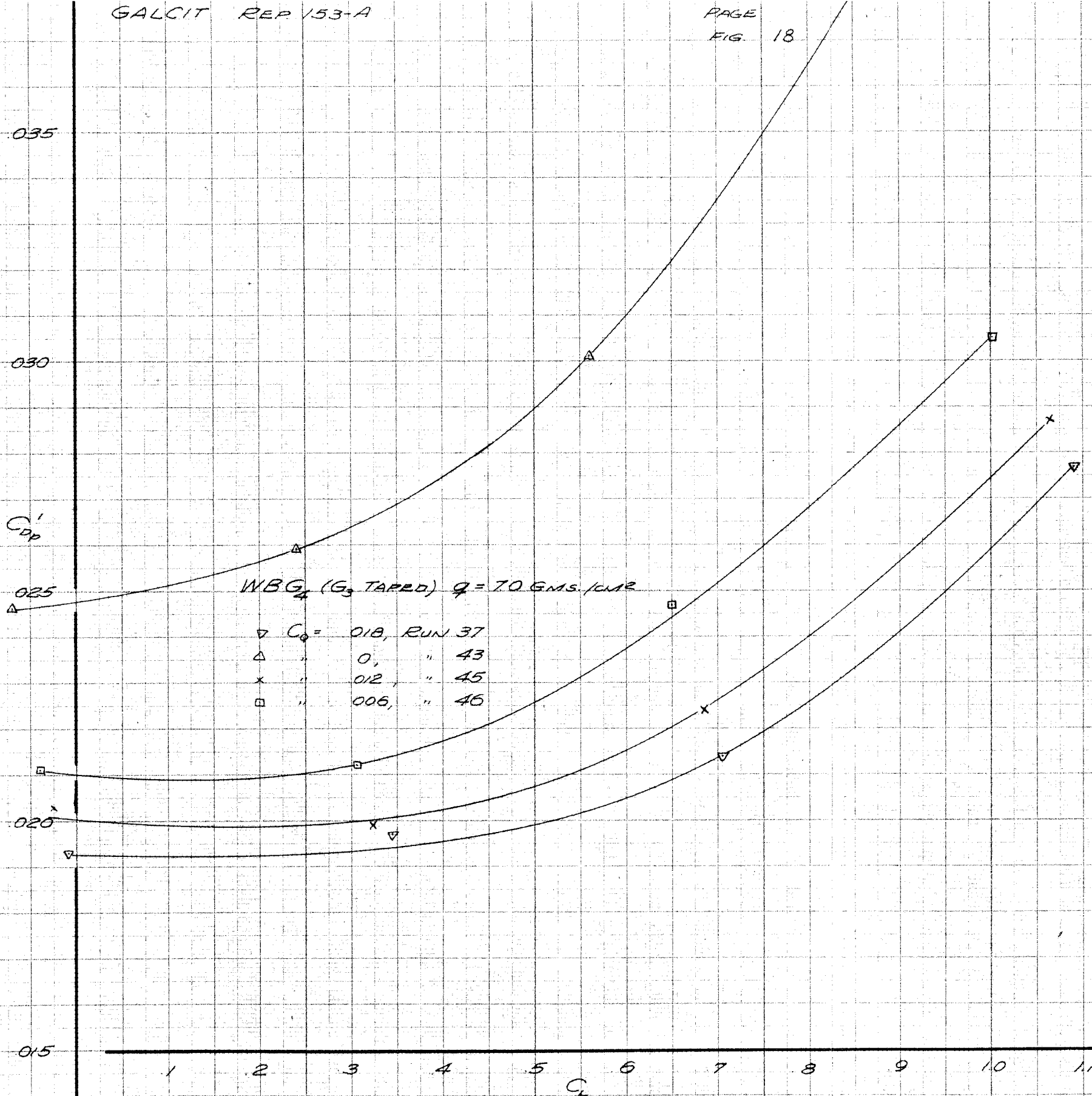
EFFECT OF SUCTION ON IDEAL PARASITE DRAG  
 $q = 25 \text{ GMS/CM}^2$

SLOT G<sub>3</sub>



EFFECT OF SUCTION ON IDEAL PARASITE DRAG  
 $q = 35 \text{ GMS./CM}^2$

SLOT  $G_3$



EFFECT OF SUCTION ON IDEAL PARASITE DRAG  
 $q = 70$  GMS./CM<sup>2</sup>  
 SLOT G<sub>4</sub>

0.35

0.30

0.25

0.20

0.15

$C_{DP}$

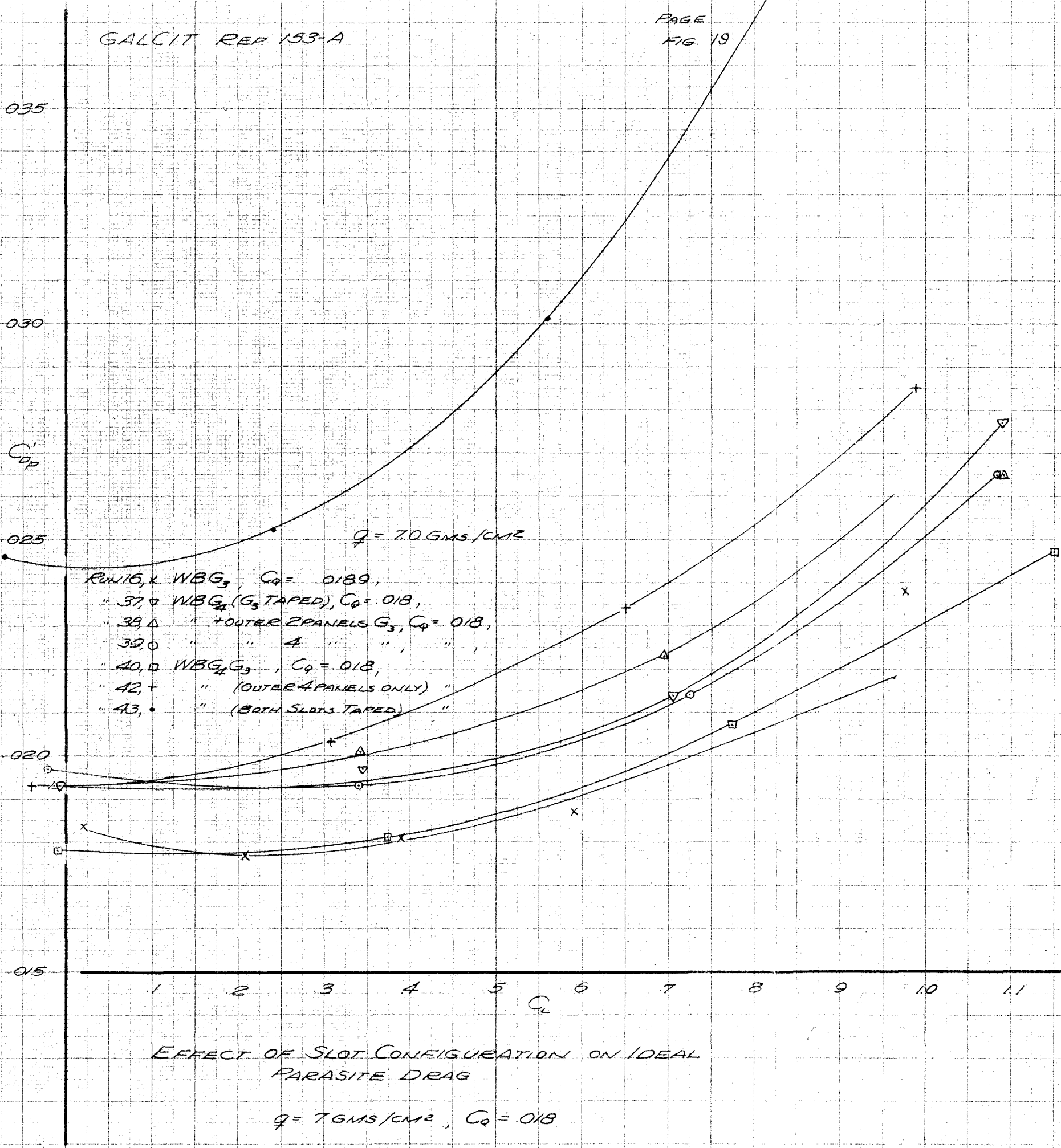
$q = 7.0 \text{ GMS/CM}^2$

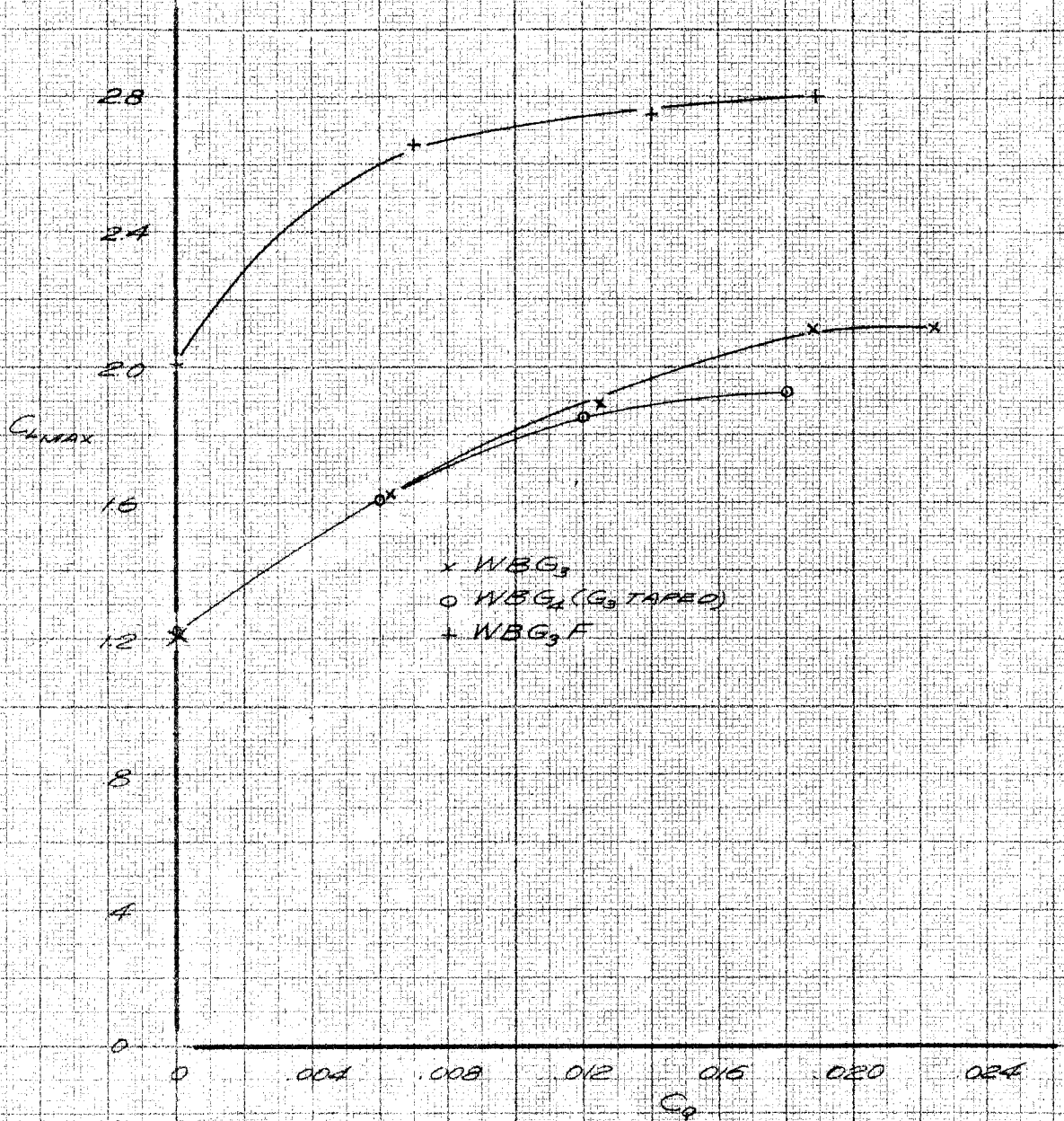
- Run 16, x WBG<sub>3</sub>,  $C_q = 0.189$ ,
- " 37, ∇ WBG<sub>4</sub> (G<sub>3</sub> TAPED),  $C_q = 0.18$ ,
- " 39, Δ " + OUTER 2 PANELS G<sub>3</sub>,  $C_q = 0.18$ ,
- " 39, ○ " " 4 " " " " " " " " " " " "
- " 40, □ WBG<sub>4</sub> G<sub>3</sub>,  $C_q = 0.18$ ,
- " 42, + " (OUTER 4 PANELS ONLY) "
- " 43, • " (BOTH SLOTS TAPED) "

1 2 3 4 5 6 7 8 9 10 11  
 $C_L$

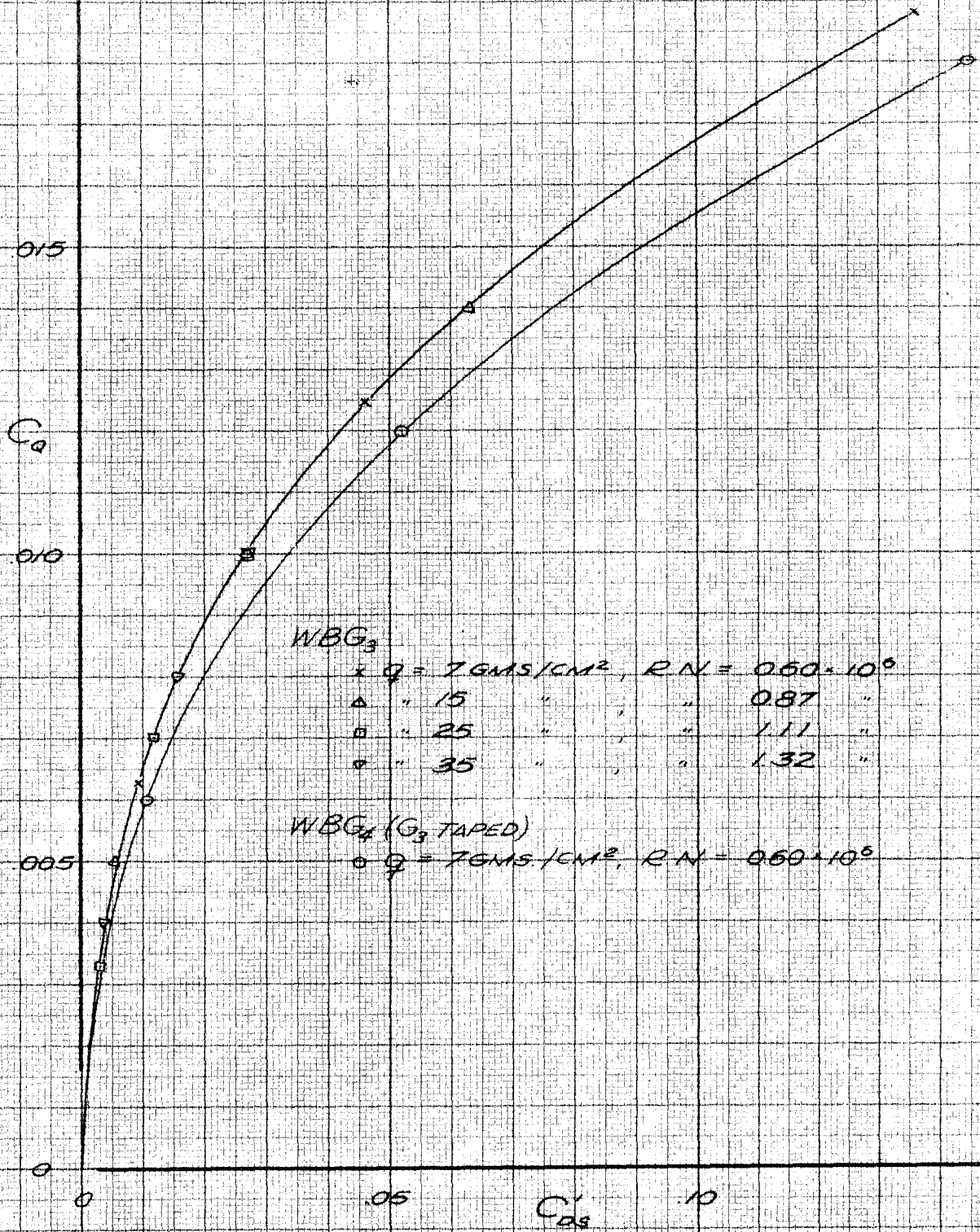
EFFECT OF SLOT CONFIGURATION ON IDEAL  
PARASITE DRAG

$q = 7 \text{ GMS/CM}^2$ ,  $C_q = 0.18$



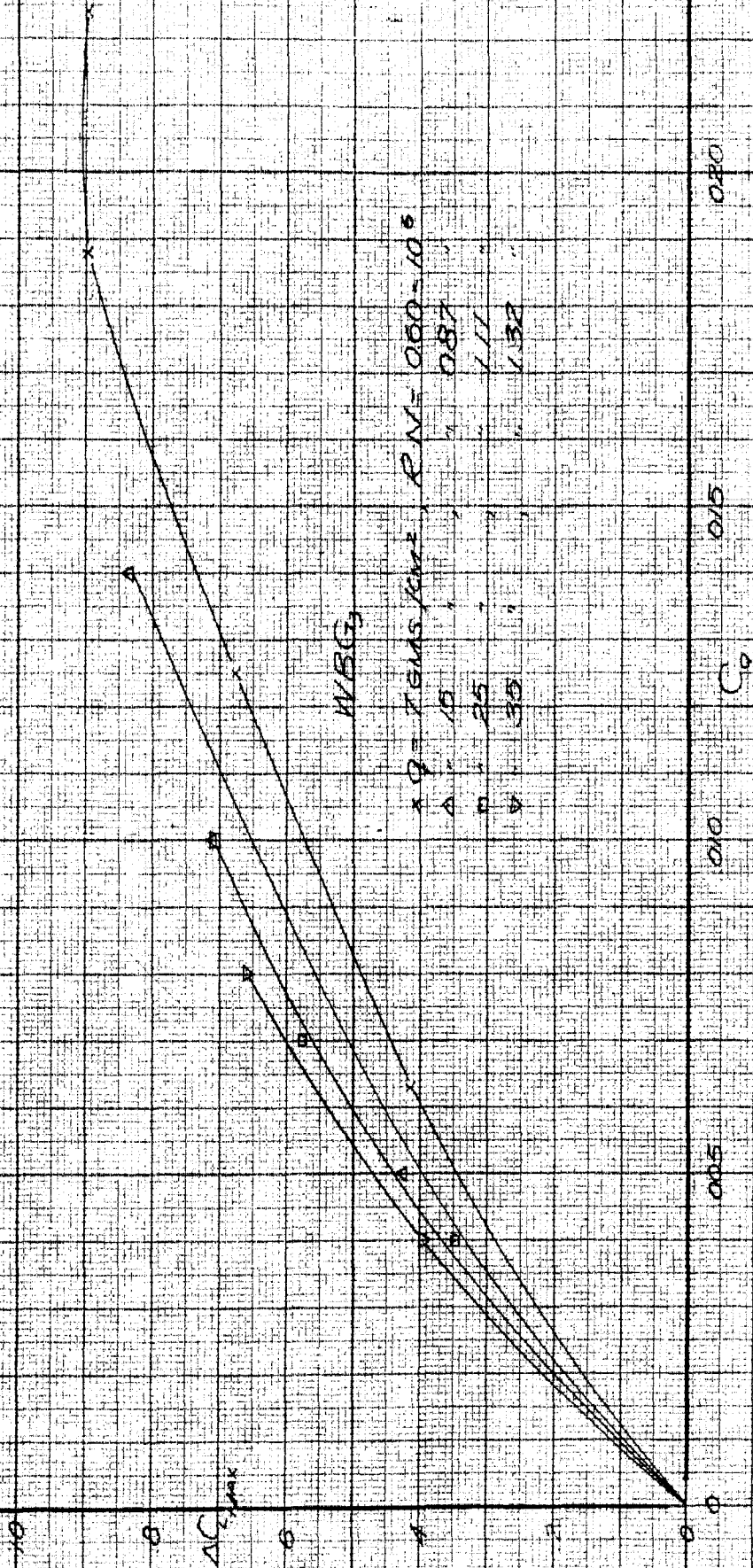


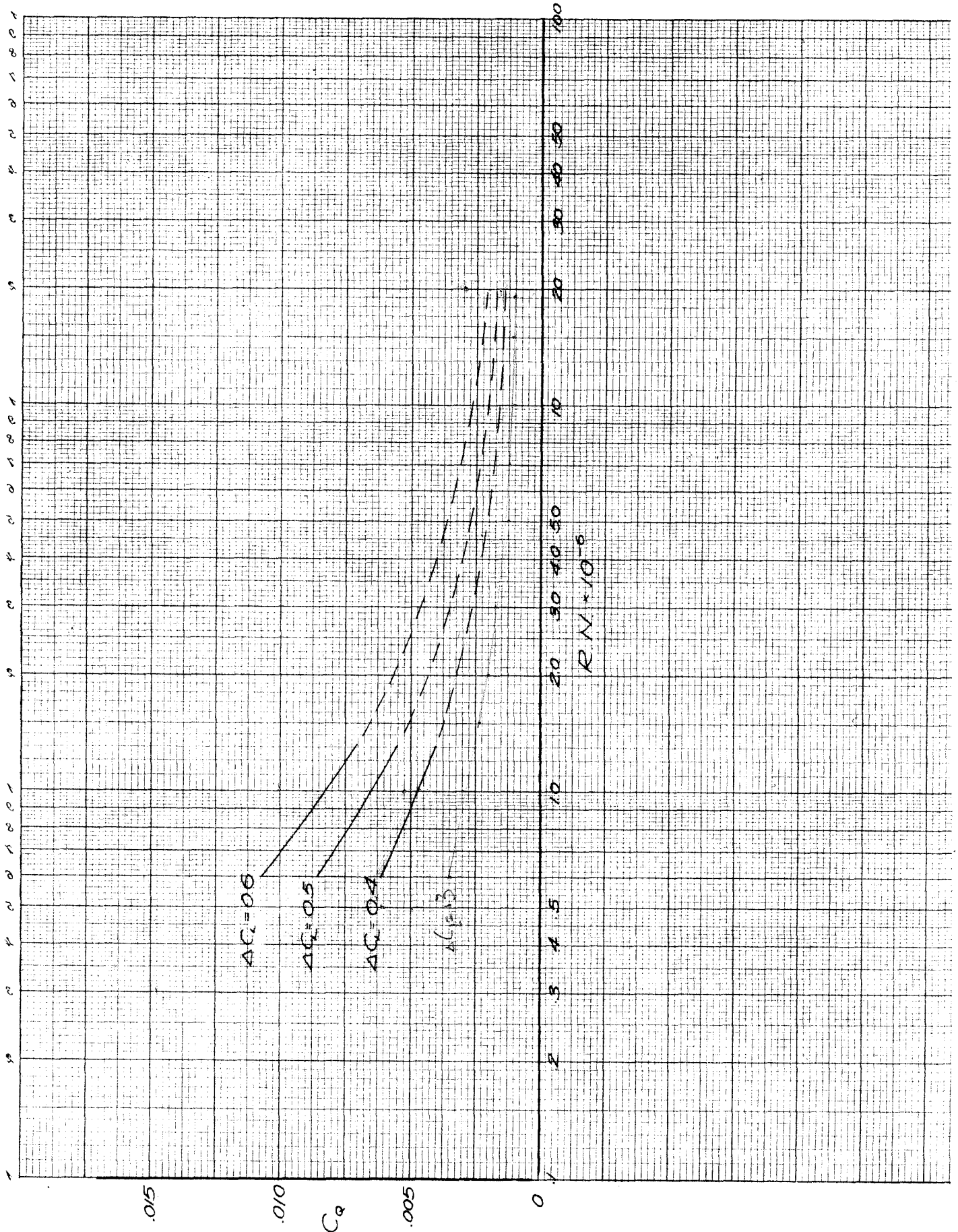
VARIATION OF MAXIMUM LIFT COEFFICIENT  
WITH SUCTION FOR VARIOUS CONFIGURATIONS



VARIATION OF POWER COEFFICIENT WITH QUANTITY COEFFICIENT FOR SLOTS  $G_3$  AND  $G_4$

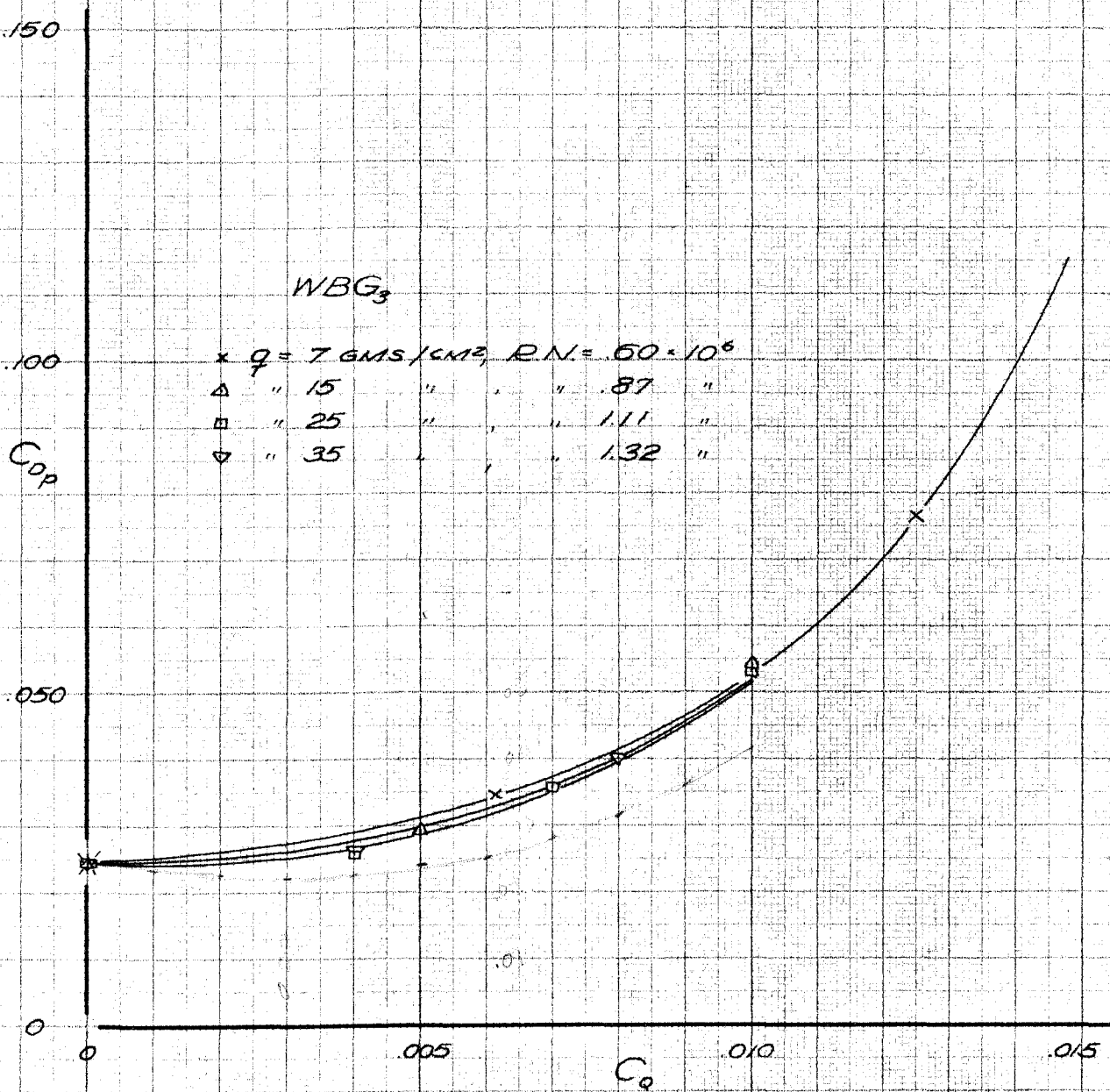
VARIATION OF LIFT INCREMENT WITH SUCTION  
FOR VARIOUS REYNOLDS NUMBERS



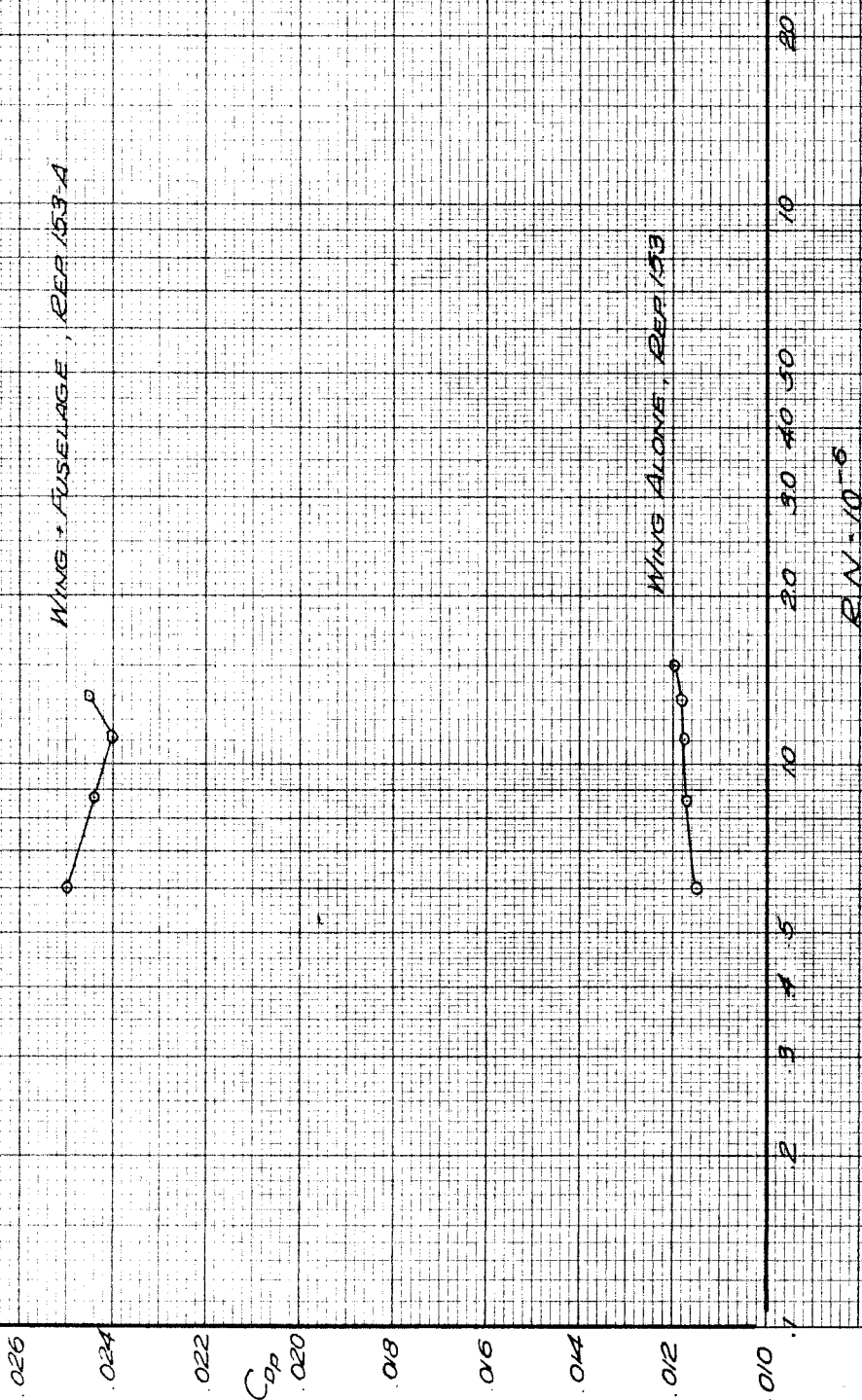


SUCTION REQUIRED TO PRODUCE A GIVEN LIFT INCREMENT AT ANY REYNOLDS NUMBER

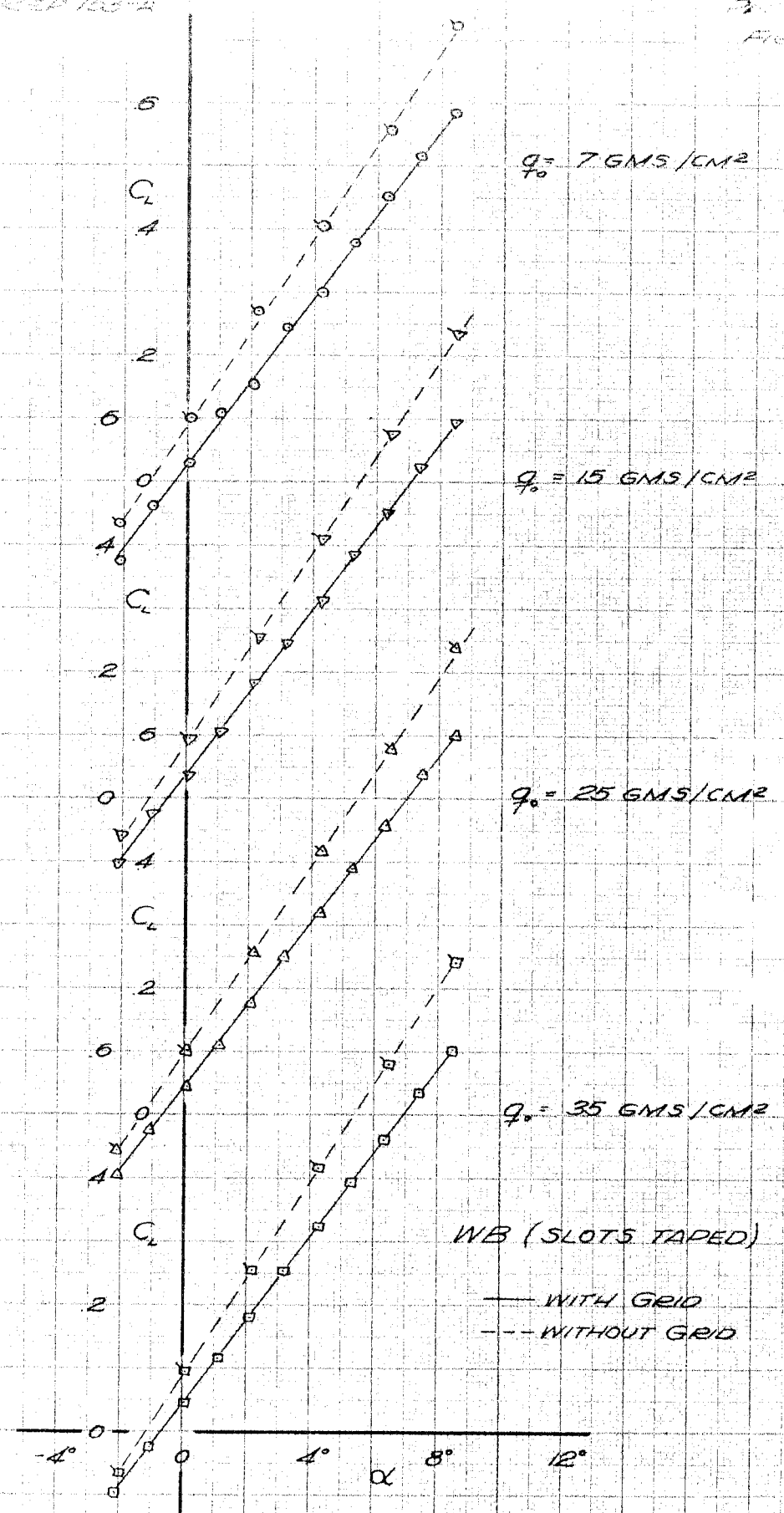




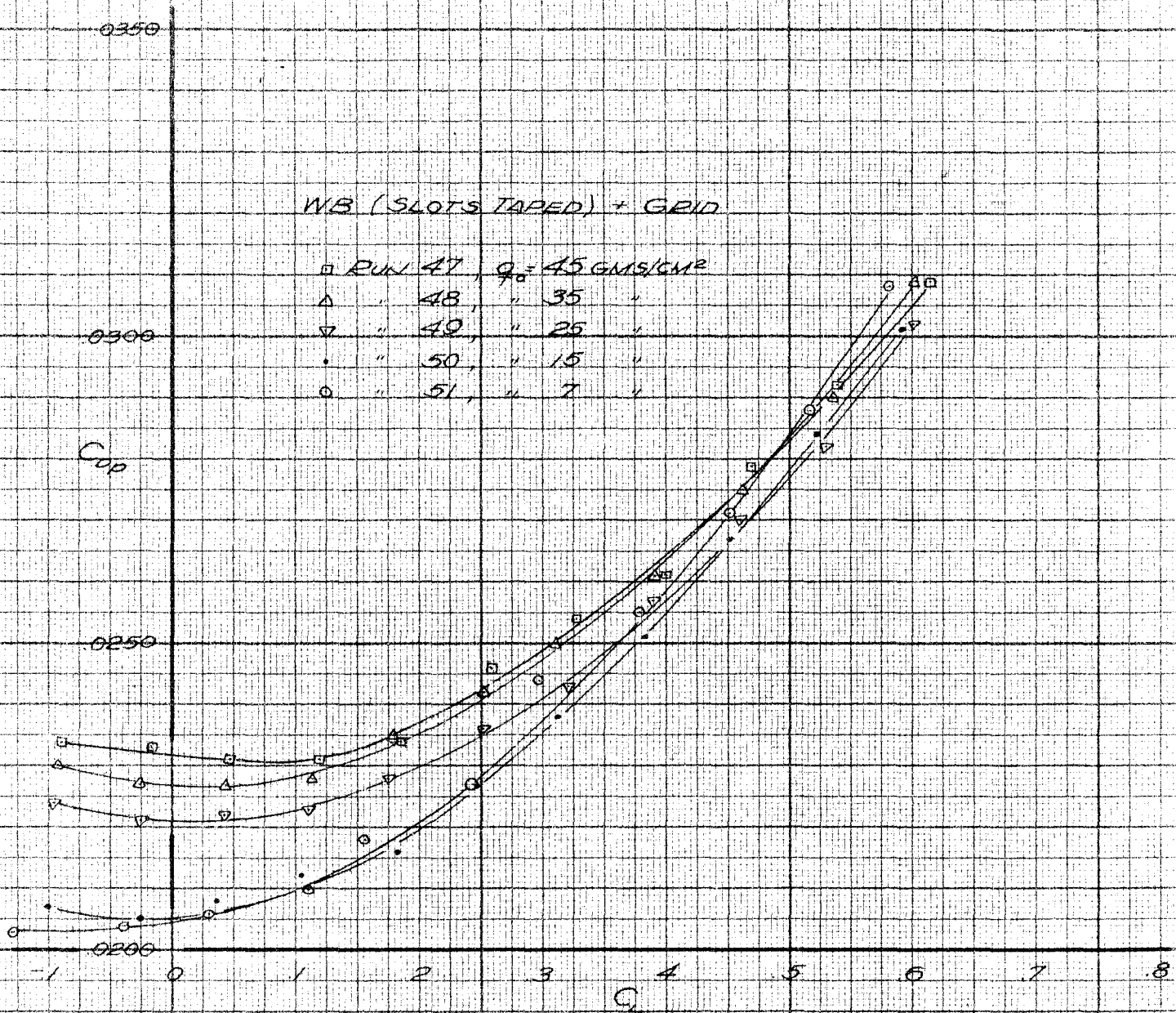
VARIATION OF EQUIVALENT PARASITE DRAG  
WITH SUCTION FOR VARIOUS R.N.'s



SCALE EFFECT ON DRAG - NO SUCTION



EFFECT OF GRID ON SLOPE OF LIFT CURVE



DRAG RESULTS BASED ON NORMAL TUNNEL  
CALIBRATION

APPENDIX I

CALCULATION OF LIFT AND MOMENT DUE TO A SINK ON THE UPPER SURFACE OF A THIN AIRFOIL

Transforming the airfoil in the z plane to a circle in the  $\zeta$  plane with the usual Joukowski transformation\*,  $z = \zeta + \frac{c^2}{\zeta}$ , where  $a = \frac{c}{4}$ , and placing a sink,  $2Q$ , at  $\zeta = ae^{i\vartheta}$  and a source,  $Q$ , at the origin, the potential function,  $\phi$ , may be written:

$$\phi = \frac{Q}{2\pi} \text{LOG } r - \frac{Q}{2\pi} \text{LOG} [r^2 + a^2 - 2ar \cos(\theta - \vartheta)]$$

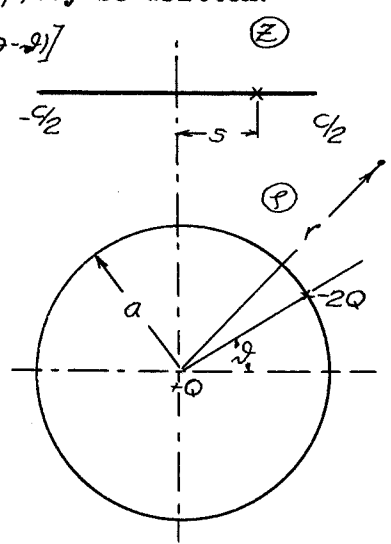
Then the radial velocity on the boundary,  $r = a$ , is given by

$$V_r \Big|_{r=a} = \frac{d\phi}{dr} \Big|_{r=a} = \frac{Q}{2\pi} \left[ \frac{1}{a} - \frac{2a - 2a \cos(\theta - \vartheta)}{2a^2 - 2a^2 \cos(\theta - \vartheta)} \right] = 0$$

and the circle is thus a streamline.

Hence the problem, as pictured above, represents the potential function for a

thin airfoil with a net sink strength,  $Q$ , on the upper surface at a distance  $s$  behind the mid-point of the airfoil. ( $\frac{s}{c/2} = \cos \vartheta$ )



LIFT INCREMENT

At  $\theta = 0$ , corresponding to the trailing edge of the airfoil, the tangential velocity is given by:

$$V_\theta \Big|_{\theta=0} = \frac{1}{a} \frac{d\phi}{d\theta} \Big|_{\theta=0} = \frac{Q}{2\pi a} \left[ \frac{2a^2 \sin(\theta - \vartheta)}{2a^2 - 2a^2 \cos(\theta - \vartheta)} \right]_{\theta=0} = \frac{Q}{2\pi a} \frac{\sin \vartheta}{1 - \cos \vartheta}$$

Assuming the Kutta condition at the trailing edge, this velocity must be cancelled by the velocity due to an increased circulation,

$\Gamma$ , whereby, equating these velocities:

$$\frac{\Gamma}{2\pi a} = \frac{Q}{2\pi a} \frac{\sin \vartheta}{1 - \cos \vartheta}$$

and the increment in lift coefficient becomes

$$\Delta C_L = \frac{\rho V \Gamma}{\rho/2 V^2 c} = \frac{2Q}{Vc} \frac{\sin \vartheta}{1 - \cos \vartheta}$$

$$\Delta C_L = 2C_Q \frac{\sin \vartheta}{1 - \cos \vartheta}$$

\* See any Standard Reference on Hydrodynamics

## MOMENT INCREMENT

From vortex sheet theory the local circulation in the real plane,  $\gamma(x)$ , is given by  $\gamma(x) = 2V_\infty(x)$ . Transforming the velocity in the  $\zeta$  plane to the  $z$  plane,  $V_\zeta = \frac{-V_\infty}{2\sin\theta}$  and substituting in the moment equation:

$$M = \int_{-\frac{c}{2}}^{\frac{c}{2}} \gamma(x) x dx$$

where  $M$  is measured positive counter-clockwise about the mid-point.

$$M = \frac{\rho V_\infty c}{2\pi a_0} \int_0^\pi \frac{\sin(\theta-\psi)}{1-\cos(\theta-\psi)} \frac{2a \cos\theta \cdot 2a \sin\theta d\theta}{\sin\theta}$$

$$M = \frac{\rho V_\infty c}{2\pi} \left[ \cos\psi \left\{ \text{LOG} \left( \frac{1+\cos\psi}{1-\cos\psi} \right) - 2 \right\} - \pi \sin\psi - 2 \sin^2\psi \right]$$

Thus the increment in moment is:

$$\Delta C_M = \frac{C_Q}{\pi} \left[ \cos\psi \left\{ \text{LOG} \left( \frac{1+\cos\psi}{1-\cos\psi} \right) - 2 \right\} - \pi \sin\psi - 2 \sin^2\psi \right]$$

## NUMERICAL VALUES:

For 70% slot:  $s = .20c$

$$\cos\psi = \frac{.20c}{c/2} = .400$$

$$\sin\psi = .916$$

$$\Delta C_L = \frac{2C_Q}{1-\cos\psi} \sin\psi = 1.53 C_Q \cdot 2$$

$$\Delta C_M = \frac{C_Q}{\pi} (-5.02) = -1.60 C_Q$$

Transferring to quarter chord point:

$$\Delta C_{M.25} = 1.22 C_Q \text{ (Positive sign now corresponds to stalling moment)}$$

For 43% slot:  $s = -.07c$

$$\cos\psi = \frac{-.07c}{c/2} = -.140$$

$$\sin\psi = .990$$

$$\Delta C_L = \frac{C_Q \cdot 2}{1-\cos\psi} \sin\psi = 0.87 C_Q \cdot 2$$

$$\Delta C_M = \frac{C_Q}{\pi} (-4.75) = -1.51 C_Q$$

Transferring to quarter chord point:

$$\Delta C_{M.25} = 1.30 C_Q$$

CHANGE IN LIFT AND MOMENT DUE TO A SHIFT IN REAR STAGNATION POINT

From two-dimensional wing theory:

$C_L = 2\pi \sin(\alpha + \beta)$  where  $\alpha$  is the angle of attack and  $\beta$  is the angle in the  $\mathcal{F}$  plane which corresponds to the position of the rear stagnation point

$$C_{M.25} = -\frac{\pi}{2} \beta$$

Assuming a small change in the location of the stagnation point corresponding to  $\Delta\beta$

$$\Delta C_{L_S} = 2\pi \Delta\beta$$

$$\Delta C_{M_S} = -\frac{\pi}{2} \Delta\beta$$

whereby:  $\Delta C_{M_S} = -\frac{\pi}{2} \frac{\Delta C_{L_S}}{2\pi} = \frac{-\Delta C_{L_S}}{4}$

To find  $\Delta C_{L_S}$ :

$\Delta S$ , the shift in the stagnation point, is given by:

$$\Delta S = \frac{c}{2} (1 - \cos \Delta\beta) \quad \text{Let } \frac{\Delta S}{c} = \frac{s}{100}$$

$$\cos \Delta\beta = 1 - \frac{2s}{100}$$

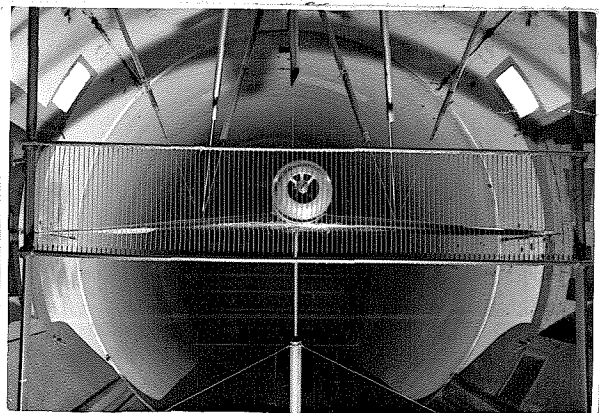
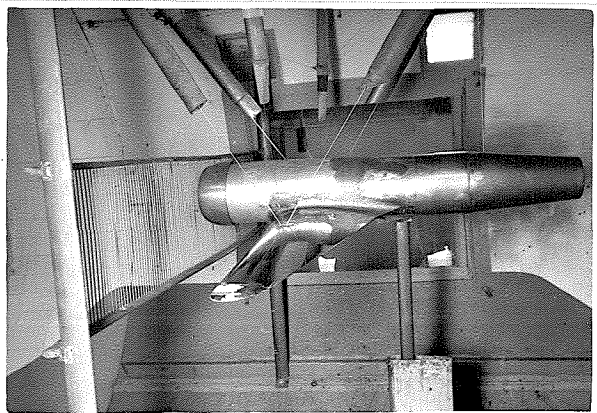
$$\sin \Delta\beta = \sqrt{1 - (1 - \frac{4s}{100} + \frac{4s^2}{100^2})} = \frac{2\sqrt{s}}{10}$$

Thus

$$\Delta C_{L_S} = \frac{2\pi \cdot 2s}{10} = .4\pi\sqrt{s}$$

## APPENDIX II

Several months after the completion of the previously described tests, which constitute this thesis, the authors were again able to put the boundary layer model in the GALCIT wind tunnel. The primary purpose of these tests was to get the model out of the transition region by introducing artificial turbulence with a grid. This was desired so that the drag data might be extrapolated to full scale. The grid was made of  $1/8$ " rods spaced  $3/4$ " apart and rigged in the tunnel as shown in the photographs.



Previous tests with this grid in the GALCIT wind tunnel\* showed that the best location for the grid was as close to the wing as possible up to approximately  $10\frac{1}{2}$ " in front of the leading edge. For this reason the grid was rigged about  $\frac{1}{2}$ " in front of the fuselage or  $12\frac{1}{2}$ " ahead of the center of the wing, which was as close to the wing as was possible.

\* See GALCIT report No. 113



A normal Reynolds Number series of runs was made with no suction and both slots taped. The results are shown in Figure 26, and it can be seen immediately that there is still a reverse Reynolds Number effect and, also, that the drag coefficient is extremely low. There are several reasons which may account for the unusual drag data.

1) The tare drags for the model with the grid installed are not accurately known.

2) There was not sufficient time to calibrate the tunnel with the grid in place and  $q$  may be appreciably in error.

3) Since the fuselage was so close to the grid, the stagnation pressure which would normally act on the front of the fuselage was taken by the grid and the fuselage was essentially in dead air behind the grid. This undoubtedly accounts for the low  $C_D$  obtained.

An attempt to correct for the reduced  $q$  behind the grid was made by comparing the slopes of the lift curves at various  $q$ 's with and without grid. These curves are given in Figure 27. It is immediately seen that the change in slope is the same at each  $q$ . Thus if the drag curves were corrected from this data the same increment in  $C_D$  would be added for each  $q$  and there would still be a reverse Reynolds Number effect.

One run was made with suction on WBG<sub>2</sub>, at  $q = 7$  and  $C_Q = .020$ , with the grid in place. The maximum lift coefficient was 1.7, as compared with 2.11 for the same case without grid. The decrease in drag due to suction was approximately the same as the case for no grid.

The authors feel that if any further attempt is to be made using a grid, the grid must be located several feet in front of the model, a tunnel calibration must be made with the grid in place, and the tare drags must be determined more accurately.